Atmos. Chem. Phys. Discuss., 12, 17607–17656, 2012
www.atmos-chem-phys-discuss.net/12/17607/2012/
doi:10.5194/acpd-12-17607-2012

Atmospheric Chemistry and Physics Discussions

Fluorescent biological aerosol particles (FBAPs) measured with the Waveband Integrated Bioaerosol Sensor WIBS-4: laboratory tests combined with a one year field study

E. Toprak and M. Schnaiter

Institute for Meteorology and Climate Research – Atmospheric Aerosol Research, Karlsruhe Institute of Technology, Karlsruhe, Germany

Received: 19 June 2012 – Accepted: 3 July 2012 – Published: 18 July 2012

Correspondence to: E. Toprak (emre.toprak@kit.edu)

Published by Copernicus Publications on behalf of the European Geosciences Union.

Abstract

In this paper bioaerosol measurements conducted with the Waveband Integrated Bioaerosol Sensor mark 4 (WIBS-4) are presented. The measurements comprise aerosol chamber characterization experiments and a one-year ambient measurement period at a semi-rural site in South Western Germany. This study aims to investigate the sensitivity of WIBS-4 to biological and non-biological aerosols, performance of WIBS-4 for discrimination of several types of aerosols, and the detection and identification of biological particles in the ambient aerosol. Several types of biological and non-biological aerosol samples including spores, bacteria, pollen, mineral dust, ammonium sulphate, combustion soot, and fluorescent polystyrene spheres were analysed by WIBS-4 in the laboratory. The results confirm the sensitivity of the Ultra Violet Light Induced Fluorescence (UV-LIF) method to biological fluorophores and show the good discrimination capabilities of the two wavelengths excitation/two wavebands detection method applied in WIBS-4. However, a weak cross-sensitivity to non-biological fluorescent interferers remains and is discussed in this paper.

All the laboratory studies have been undertaken in order to prepare WIBS-4 for ambient aerosol measurements. According to the one year ambient aerosol study, number concentration of fluorescent biological aerosol particles (FBAP) show strong seasonal and diurnal variability. The highest number concentration of FBAP was measured during the summer term and it decreases towards the winter period when colder and drier conditions are prevailing. Diurnal FBAP concentrations start to increase after sunset and reach maximum values during the late night and early morning hours. On the other hand the total aerosol number concentration was always higher during day time than during night time and a sharp decrease after sunset was observed. There was no correlation observed between the FBAP concentration and the meteorological parameters temperature, precipitation, wind direction and wind speed. However a clear correlation was identified between the FBAP number concentration and the relative

ACPD

12, 17607–17656, 2012

humidity. Humidity controlled release mechanisms of some fungal spore species are discussed as a possible explanation.

1 Introduction

Primary biological aerosol particles (PBAPs) basically consist of solid particles that are derived from living organisms, including microorganisms, dispersal units and fragments of all varieties of living things and they can be either dead or alive (Despres et al., 2012). This subset of the atmospheric aerosol contains fungi, viruses, bacteria, spores, pollens and animal and plant debris. PBAPs are potentially important for cloud formation processes because they have the potential to act as effective cloud condensation nuclei (CCN) and heterogeneous ice nuclei (IN) at temperatures as warm as −2 °C (Diehl et al., 2001, 2002). They affect the public health and play important roles in several atmospheric processes (Pöschl, 2005). There are not enough studies yet about the abundance of PBAPs in the atmosphere, their release and dispersal mechanisms and their role in atmospheric aerosol – cloud processes.

Previous studies that have been conducted over the past 10 yr have shown that atmospheric PBAP concentrations are highly variable and strongly related to the biological activity in the measurement area (Matthias-Maser et al., 1995; Matthias-Maser and Jaenicke, 1995). Because of the lack of online measurement systems, the PBAP budgets have been estimated by mainly using proxy measurements such as Mannitol and organic carbon (Elbert et al., 2007). Electron microscopy investigations combined with EDX analysis of atmospheric samples have revealed a PBAP to total coarse mode aerosol particle ratio of 23.7 % in an urban/rural area and 19.5 % at a remote continental area, which correspond to PBAP number concentrations of 1.9 and 0.22 cm^{-3}, respectively (Matthias-Maser et al., 2000). It should be noted that these numbers refer only to a specific size range. Gruber et al. (1999) collected both marine and continental air samples on Helgoland, Germany and on board of an aircraft over the North Sea. They analysed concentration and the chemical composition of aerosol in marine and

ACPD
12, 17607–17656, 2012

continental air and found that the fraction of biological particles in the total aerosol load is around 20 % for continental areas, while in marine air this value was determined to be around 9 %. Jaenicke (2005, 2007) found coarse mode PBAP number concentrations between 1–3 cm^{-3} (3–50 %) in Mainz and between 0.1–1 cm^{-3} (15–30 %) at Lake Baikal.

Yadav et al. (2004) studied bacterial colonization and report phyllosphere bacterial population from non-detectable up to a maximum 1.4×10^7 cells g^{-1}. Another study gives average population densities of these epiphytic bacteria between 10^4 and 10^8 cells cm^{-2} (Morris and Klinkel, 2002). Christner et al. (2008) examined the DNA-containing cell concentrations and ice nuclei (IN) properties of 19 fresh snowfalls (> −10 °C) and report cell concentrations between 1.5×10^4 and 5.4×10^6 cells l^{-1} for melted snow water. The differences between the reported concentrations demonstrate the difficulty in estimating total concentrations of PBAP. Sanchez-Ochoa et al. (2007) found airborne plant debris concentrations between 0.03–0.36 µg m^{-3}. The bacterial mass concentration was reported around 0.1 µg m^{-3} (Bauer et al., 2002; Burrows et al., 2009).

In addition, there are studies dealing with the release and detection of fungal spores. Bauer et al. (2002) for instance examined the number concentration of fungi at a continental background in Austrian Alps and reported fungal spore concentrations around 7.3×10^2 spores m^{-3}. Gilbert and Reynolds (2005) counted fungal spores in a tropical forest and reported diurnal concentrations ranging from $\sim 10^2$ spores l^{-1} to $\sim 10^3$ spores l^{-1}. Wu et al. (2004) reported a total fungal spore concentration of 28 spores l^{-1} in Southern Taiwan and added that increasing daily temperature and relative humidity is associated with rising Basidiospore levels in the atmosphere. They also concluded that increasing Basidiospore levels in sandstorm days are mainly allocable to the dust event in that area.

Fungal spores are indeed a significant fraction of the atmospheric PBAP (Womiloju et al., 2003; Elbert et al., 2007; Bauer et al., 2008; Crawford et al., 2009). *Basidiomycota* (BMC), which can release their spores according to active and passive

ACPD
12, 17607–17656, 2012

mechanisms and have higher abundances at night, is one of the most abundant classes in fungi. This class of fungal spores comprise rusts, smuts and most mushroom forming fungi that produce a diverse array of fruiting bodies (Fröhlich-Nowoisky et al., 2012). The abundance of fungal spores shows differences due to the environmental factors such as measurement location, season, measurement time and weather conditions (Elbert et al., 2007). The release of actively wet discharged *Basidiomycota* (BMC) appears to be correlated to the relative humidity instead of precipitation (Hirst, 1953; Gregory and Hirst, 1957; De Antoni Zoppas et al., 2006).

The online methods, which are developed in response to bio-warfare agents, made the detection of bioaerosols from the ambient atmosphere available (Pinnick et al., 1998; Hill et al., 1999, 2001). The Ultraviolet Aerodynamic Particle Sizer (UV-APS) is the first commercially available instrument being able to detect bioaerosols (Hairston et al., 1997; Brosseau et al., 2000). Huffman et al. (2010) gave an overview of the abundance of FBAP in Mainz, Germany by using the UV-APS. They analysed the particles having an aerodynamic particle size $1.0\,\mu m < Da < 20\,\mu m$ and found that FBAP size distribution had shown a strong diurnal cycle with a dominant peak around 3–4 µm, which could be attributed to fungal spores or agglomerated bacterial cells. They also reported the highest number concentration in September between 8×10^3 and $1.2 \times 10^4\,l^{-1}$ for total aerosol and around $8.5 \times 10^2\,l^{-1}$ for fluorescent particles, respectively. Average FBAP number and mass concentrations were reported to be around $27\,l^{-1}$ and $1.3\,\mu g\,m^{-3}$, respectively. Gabey et al. (2010, 2011) used the Waveband Integrated Bioaerosol Sensor mark 3 (WIBS-3) to measure fluorescent biological aerosol particles in a tropical rainforest and compared the results with equivalent measurements at an urban area in Manchester. They found the minimum and the maximum FBAP number concentrations in the understory as $50–100\,l^{-1}$ late in the morning and $4 \times 10^3\,l^{-1}$ in mid-afternoon, respectively. The FBAP number concentrations between midnight and sunrise were reported between 10^3–$2.5 \times 10^3\,l^{-1}$. On the other hand, a strong fluctuation was seen for the above canopy FBAP number concentrations, which were reported as $50–100\,l^{-1}$ during day time and $200–400\,l^{-1}$ at night. They

ACPD
12, 17607–17656, 2012

also attributed these strong FBAP fluctuations to the release of fungal spores below the canopy and appeared to be linked to the elevated relative humidity of the medium.

In this paper, we present online measurements of ambient FBAP by using the latest version of the WIBS instrument suite (WIBS-4), which is based on the UV Light Induced Fluorescence (UV-LIF) method. To our knowledge this is the first online FBAP study that covers a complete seasonal cycle. Although previous studies by Gabey et al. (2010, 2011) and Huffman et al. (2010) measured online ambient FBAP concentrations, their studies cover only short periods and do not provide any information about the seasonal behaviour of the biological aerosol. Gabey et al. (2010) sampled the fluorescent biological aerosol particles for 10.5 days (from 19 April to 3 May 2008) and for 75 h (from 18–23 July 2008). Gabey et al. (2011) collected fluorescent data from 4–21 December 2009. Huffman et al. (2010) collected the ambient data from 3 August to 4 December 2006. Our data give an insight on how the PBAP concentration differs in time and also gives first correlations of the PBAP budget with the meteorological conditions. We found especially a significant correlation of the FPAB concentration with the relative humidity. Our results contribute to the recent discussions on the role of PBAP for atmospheric processes and might be a useful data set for the development of new PBAP emission parameterizations for atmospheric aerosol and cloud models.

2 Experimental methods

The UV-LIF method is used in this study for the discrimination of non-biological aerosol from biological aerosol particles (Pinnick et al., 1995; Hairston et al., 1997; Eversole et al., 2001; Ho, 2002). The method is focused on detecting the fluorescence signals from common amino acids like tryptophan, phenylalanine and tyrosine and also from nicotinamide adenine dinucleotide (NADH), which is the metabolic product of bacteria. Among the 20 amino acids, these three are the only ones that can produce enough intrinsic fluorescence after being treated by UV light. Tryptophan is the only amino acid that shows fluorescence emission between 300–450 nm (excitation at 280 nm) and its

ACPD
12, 17607–17656, 2012

emission signal is not absorbed by other species (Pan et al., 2007; Pöhlker et al., 2012). NADH is another bio-molecule which is ubiquitous among living organisms with a fluorescence emission between 400–600 nm (excitation at 370 nm, Pöhlker et al., 2012). The combination of measured fluorescence signals from tryptophan and NADH makes it possible to analyse and differentiate biological aerosol with this method.

2.1 WIBS-4 technical details

WIBS-3 is a single aerosol particle fluorescence monitor that uses the Ultra Violet Light Induced Fluorescence (UV-LIF) method to detect FBAP (Kaye et al., 2005; Foot et al., 2008; Stanley et al., 2011). WIBS-4 incorporates numerous software improvements over previous WIBS versions as well as a five-fold improvement on fluorescence sensitivity. In principle WIBS-4 has two filtered Xenon lamps, which provide two sequential ultraviolet pulses centred at 280 and 370 nm. The Xenon lamps are capable of firing at a maximum repetition rate of approximately 125 Hz. This corresponds to a maximum detectable particle concentration of approximately 2×10^4 particles l^{-1}. These ultraviolet pulses are used to excite tryptophan and NADH fluorescence in the particles. Resulting total fluorescence is then measured in three fluorescence channels: the emission following a 280 nm excitation is recorded in the 310–400 nm (channel F1, tryptophan) and 420–650 nm (channel F2) wavebands, and a 370 nm excitation is recorded in the 420–650 nm waveband (channel F3, NADH). These individual channels provide essential information about the nature of the detected particles. Therefore, as in the previous study by Gabey et al. (2010) we also used the combination of F1 and F3 for discriminating fluorescent biological aerosol particles (FBAP). As in the previous WIBS instruments, the Mark 4 version records the optical size and the shape in addition to the fluorescence excitation-emission matrix from individual particles collected in the approximate size range 0.5–16 µm. Owing to possible interference from non-biological fluorescent particles (generally consist of particles <0.8 µm) we calculated the total (N_T) and the fluorescent biological aerosol number concentrations (N_{FBAP}) for particles

ACPD
12, 17607–17656, 2012

in the size range $0.8 < D_p < 16\,\mu m$. The cross-sensitivity issue is discussed in Sect. 2.2 in detail.

WIBS-4 detects forward scattered light using a quadrant photomultiplier tube (PMT). The four scattering signals of this detector are used to size the particles according to Mie theory and to deduce information about the particle shape. The latter is based on the fact that only spherical particles scatter light axisymmetric around the incident light direction while non-spherical particles in general show an asymmetric scattering pattern. Therefore, it is possible to find a metric relation between particle shape and the azimuthal distribution of the scattered light, which is defined as the Asymmetry Factor AF (Hirst et al., 2001; Kaye et al., 2007).

$$\mathrm{AF} = \frac{k\left(\sum_{i=1}^{n}\left(\bar{E} - E_i\right)^2\right)^{1/2}}{\bar{E}} \quad (1)$$

Here, $\bar{E}$ is the mean of the four scattering intensities of the quadrant PMT and k is an instrument constant to ensure that the maximum possible value of AF is 100. According to this definition, AF is zero for a perfectly spherical particle, while it approaches to 100 for a fibre which is oriented with its long axis perpendicular to the incident light direction. It was found by Foot et al. (2008) that an elongated particle, such a rod-shaped substance, indeed tends to be aligned parallel to the direction of the sample airflow, i.e. perpendicular to the incident light. In laboratory tests with polystyrene latex (PSL) particles, we have found that due to the detector noise the AF value of real spherical particles is around 8 with slightly higher values for particles with diameters at the lower detection limit of the instrument (Fig. 1).

As for other optical particle counters, the WIBS-4 scattering channel is calibrated by using spherical PSL particles of known diameter and refractive index. In the present work the manufacturer instrument calibration was checked from time to time with PSL particles of different size.

ACPD
12, 17607–17656, 2012

The total aerosol flow for WIBS-4 is set to 2.5 l min^{-1}. A special aerosol inlet system is used in WIBS-4 in order to generate a confined particle beam through the detection volume. For that, the total aerosol flow is split and the main part is directed through a HEPA filter and then returned to sheath the remaining sample flow in the inlet. In this way a confined sample flow of about 0.23 l min^{-1} is generated by the inlet.

2.2 Fluorescence threshold for identification of FBAP

With each UV excitation pulse, the WIBS-4 records always a finite amount of background fluorescence. To distinguish this background from the particle-induced fluorescence signal a threshold is defined. Therefore, the instrument can be operated in a forced trigger mode, to measure solely the background fluorescence. In this mode the xenon lamps are fired periodically at approximately 1 s intervals with no particles present. A minimum 5 min forced trigger measurement was always performed before starting any measurement.

Background fluorescence intensity in each channel (F1, F2, and F3) is a combination of the standard deviation of detector noise, the variability of the UV pulse intensities, and the fluorescence induced from aerosol particles escaped from the aerosol flow and deposited on the inner walls of the detection chamber. Following Gabey et al. (2010), the noise threshold is defined as in Eq. (2) and could be altered during data processing. Forced trigger data are marked in the single particle data set. According to Eq. (2), any measured fluorescence signal having an intensity above $E_{\text{Threshold}}$ is accepted and recorded as a fluorescent particle.

$$E_{\text{Threshold}} = \bar{E}_i + 3\sigma_i \quad (i = \text{fluorescence channels}) \tag{2}$$

For the one year ambient operation of WIBS-4, the variability of the background fluorescence signals of the individual channels is shown on Fig. 2. From these measurements the mean background signals $\bar{E}_i$ and standard deviations σ_i were determined for the three fluorescence channels as 39.02 ± 1.92 for F1_280, 6.33 ± 2.82 for FL2_280, and

ACPD
12, 17607–17656, 2012

37.84 ± 4.48 for FL2_370, in arbitrary units. Stability of the power of UV lamps was also checked and despite a slight increase of Xe-280 (~12.5 %) and Xe-370 (~8 %) intensities with time, neither sudden increase nor decrease was observed.

In the UV-LIF method approximately 1 % of non-fluorescent particles are misclassified as fluorescent, but an unknown number of fluorescent particles inevitably go undetected through the pre-defined threshold levels of the instrument (Gabey et al., 2010). Moreover, there is another class of aerosol which consists of substances having fluorescent ability although they are non-biological in nature. This is well known as interference to UV-LIF detection. Since they produce high fluorescence intensities on different channels, it is difficult to exclude this kind of fluorescence signal from the total fluorescence.

However, as an advantage of single particle detection, a variable threshold value can be described and used. Laboratory analysis of several biological and non-biological aerosols gives an idea about fluorescence behaviour of non-biological aerosols. It was shown that these particles produce sparse false triggers that saturate the fluorescence detectors, especially under high aerosol concentrations. On the other hand it could be shown that typical biological aerosol particles, e.g. bacteria and spores, never saturate the fluorescence detectors. Hence our new threshold analysis also excludes particles showing fluorescence signal high enough to saturate the detectors in addition to those particle events that can be excluded according to the lower threshold definition given in Eq. (2). However, a remaining low fraction of the non-biological aerosol particles might still be misclassified. The contribution of those particles to the FBAP aerosol fraction must be quantified by laboratory studies.

2.3 Data analysis methods

The instrument is controlled via a laptop connected over a USB 2.0 port. Manufacturers' software is used to store the measured single particle data in comma separated value (CSV) files. The CSV files contain the particle arrival time, the forward and side scattering data, the power of the xenon lamps, the fluorescence intensities for the three

ACPD
12, 17607–17656, 2012

different channels, the time of flight (TOF) values, the particle optical size in µm, the asymmetry factor values as well as the missed particle counts.

A Matlab program is used to process the single particle data. The program was written and applied for WIBS-3 data in previously published studies (Gabey et al., 2010, 2011). Because of the huge amount of single particle data, the data sets were binned into 15 min time bins and analysed. The Matlab code searches through all data and collects the marked forced trigger data for each individual channel and calculates $\bar{E}_i$ and σ_i values for the individual channels (cf. Sect. 2.2). According to Eq. (2), the threshold intensity is calculated ($E_{\text{Threshold}}$) and all single particles having a fluorescence signal above this threshold value and not saturating any fluorescence channel are accepted as fluorescent aerosol particles.

3 Result and discussion

3.1 Laboratory aerosol tests

The experiments were conducted at the stainless steel aerosol chamber NAUA at the Institute for Meteorology and Climate Research (IMK-AAF, KIT). The experiments were conducted within the large international campaign BIO-05, which had the focus on the role of biological aerosols on cloud formation and ice nucleation. The chamber has a volume of 3.7 m^3 and is equipped with a comprehensive set of aerosol instruments. Number concentration and size distribution of the aerosol in the chamber were measured by the set of devices including the WIBS-4, an Aerodynamic Particle Sizer (APS, TSI mod. 3321) as well as a Condensation Particle Counter (CPC, TSI mod. 3022, 3775).

Because the WIBS-4 detection method is based on the measurement of intrinsic fluorescence from single atmospheric aerosol particles, it is likely that there are non-biological components in the atmospheric aerosol that show a detectable amount of fluorescence signal. For instance, soot particles from combustion processes, which

ACPD
12, 17607–17656, 2012

contain Polycyclic Aromatic Hydrocarbon (PAH) components, contribute to the $PM_{2.5}$ mass of the atmospheric aerosol (Schauer et al., 2004). These aerosol components show fluorescence emission after the excitation with UV light (Pöhlker et al., 2012). Several laboratory experiments were performed in this study to investigate the efficiency of WIBS-4 for discriminating biological aerosol from non-biological aerosol. Several main atmospheric aerosol components including ammonium sulphate, black carbon, cellulose fibres, and mineral dusts were used in these experiments. Based on the results of these laboratory tests it is possible to optimise the threshold detection levels of WIBS-4 in order to get a good discrimination of non-biological and biological aerosol particles (cf. Sect. 2.2). This optimisation is a trade-off between higher threshold values, which can cause a non-detection of some biological aerosol species and relatively low thresholds, which can cause a significant misclassification of non-biological particles.

3.1.1 Ammonium sulphate and fungal spores

Figure 3 shows the number and size distributions of mixture of two atmospheric aerosols, which were measured by WIBS-4 from the NAUA chamber. First, ammonium sulphate aerosol was added to the chamber until the number concentration measured by the CPC reached an initial value around $5 \times 10^4\,l^{-1}$. The ammonium sulphate aerosol had been sampled for approximately 80 min before about $2 \times 10^4\,l^{-1}$ of *penicillium notatum* type of spores were added. At that time the CPC number concentration of the ammonium sulphate particles had already dropped to about $2.5 \times 10^4\,l^{-1}$. The time evolution of the experiment is illustrated by Fig. 3. Because of the different size ranges of the CPC and WIBS-4 instruments, the total number concentration measured by WIBS-4 for the ammonium sulphate aerosol was only around $0.4 \times 10^4\,l^{-1}$.

The FBAP number concentrations deduced from the WIBS-4 fluorescence data for spores and ammonium sulphate aerosols were around $1.0 \times 10^3\,l^{-1}$ and below $10\,l^{-1}$, respectively. The FBAP to total aerosol ratio was calculated as 0.1 % for ammonium sulphate and around 20 % for spores. If WIBS-4 would have classified all the fungal

ACPD
12, 17607–17656, 2012

spores ($\sim 2 \times 10^4\ l^{-1}$) in the chamber as biological, $N_{FBAP} N_T^{-1}$ ratio would be about 80 %. However, $N_{FBAP} N_T^{-1}$ ratio stayed around 20 %. This result can be explained by considering that our definition of biological aerosol consists of only viable species. To find the quantitative contribution of the particle fluorescence to the number of biological particles, which is calculated by using different definitions of biological aerosol, Fig. 3a, b is represented side by side. By comparing panels (a) and (b) of Fig. 3, it can be seen that the FBAP definition given in Table 1 results in a much better discrimination of the biological particles. Figure 3a shows that ammonium sulphate aerosol produces a fluorescence signal mainly in channel F1, which is the short wavelength excitation and detection. On the other hand using a combination of the two fluorescence detection channels F1 and F3 suppresses almost all ammonium sulphate aerosol particles in the fluorescence measurements in the case of *penicillium notatum*/ammonium sulphate mixture (Fig. 3b).

3.1.2 Mineral dust

Mineral dust is also one of the most abundant aerosols in the atmosphere (Rosenfeld et al., 2008; Monks et al., 2009) and its fluorescence ability might be the strongest interference factor of the UV-LIF method. To investigate the fluorescence behaviour of mineral dust, a series of experiments with mineral dust aerosol was performed during BIO-05. Because of its atmospheric relevance, a Saharan dust sample was used. The initial CPC number concentration after the addition of the dust was about $55\ cm^{-3}$. The Saharan dust sample that we used in the chamber had a size distribution between 0.05–2.5 µm (Möhler et al., 2006). Because of the fact that the WIBS-4 can measure the optical particle size for only particles greater than 0.5 µm, we observed a lower total aerosol number concentration compared to the CPC measurement. Therefore, Fig. 4 represents only the particles corresponding to an optical size between 0.8 and 16 µm. The total aerosol number concentration N_T was measured to be between 2×10^3 and $6 \times 10^3\ l^{-1}$.

ACPD
12, 17607–17656, 2012

We did the same analysis as in the ammonium sulphate case and compared the number concentrations of Saharan dust aerosols for different definitions of biological aerosol. Figure 4a shows the number of fluorescent particles using channel F1, while Fig. 4b represents the combination of F1 and F3 channels. Number concentrations of Saharan dust aerosol by using channel F1 was found to be between 10^2 to $10^3\,l^{-1}$, while the FBAP number concentration derived from both F1 and F3 varied between 10^1 to $10^2\,l^{-1}$. Although it was not possible to supress all Saharan dust particles as in the case of ammonium sulphate aerosol, the use of FBAP for discrimination of biological aerosol resulted in a lower contribution from Saharan dust particles. The fluorescent to total aerosol number concentration ratio ($N_{F1}\,N_T^{-1}$) was around 10 % when using the F1 channel, while $N_{FBAP}\,N_T^{-1}$ was only around 1 %. If we assume an extreme case of an ambient dust aerosol number concentration of 600 particles l^{-1}, which corresponds to a typical total aerosol concentration at our sampling site (Table 1), the mineral dust aerosol would contribute by less than 6 particles l^{-1} to the biological aerosol number concentration.

Nevertheless, the nature of the observed fluorescence behaviour of Saharan dust is quite interesting. Recent studies show that biological substances attached to dust particles can travel over long distances and therefore, strong sand storms might disperse viable microbes over wide continental regions (Hallar et al., 2011) or even globally (Smith et al., 2011). In this context we can speculate that, Fig. 4b can be either the result of a misclassification in which mineral dust particles produce false triggers or could be the first indication of microorganisms on the dust particles, which can produce true signals. In our case, it was not possible to clarify this behaviour by using the available measurements. However, this will be the subject of forthcoming studies.

3.1.3 Soot aerosol

Soot aerosol (black carbon), which is emitted through combustion processes, contributes to atmospheric aerosol and its major sources are fossil fuel and biomass

ACPD
12, 17607–17656, 2012

burning (Cooke et al., 1999). Past studies report that soot aerosol contains fluorescent Polycyclic Aromatic Hydrocarbons (PAH) and therefore, might be a significant interference factor for the UV-LIF method to detect biological particles (Schauer et al., 2004; Gabey et al., 2011; Pöhlker et al., 2012). We used aerosol emissions from a propane diffusion flame (mini-CAST, Jing Ltd, Switzerland) to investigate the WIBS-4 fluorescence detection behaviour in case of fossil fuel combustion aerosol. The CAST burner can be operated under different fuel-to-oxygen (C/O) ratios in order to generate soot aerosol emissions with different organic carbon contents (Schnaiter et al., 2006). During the BIO-05 campaign, we used CAST combustion aerosol that was generated at a C/O ratio of 0.5. The soot aerosol was mixed with ammonium sulphate aerosol in the NAUA aerosol chamber. The initial CPC aerosol number concentration of the mixture was around $1.7 \times 10^5\,l^{-1}$, which dropped to around $1.0 \times 10^5\,l^{-1}$ over the course of the experiment mainly due to dilution. The total aerosol number concentration of the particles with optical diameters larger than 0.8 µm, as measured by the WIBS-4 instrument, was around $5.0 \times 10^3\,l^{-1}$.

The time evolution of the experiment is again illustrated in the same way as the previous experiments (Fig. 5). By using the combination of F1 and F3 fluorescent channels, the N_{FBAP} was found around $10\,l^{-1}$ for ammonium sulphate and soot aerosol mixture. $N_{F1}\,N_T^{-1}$ and $N_{FBAP}\,N_T^{-1}$ were found around 1.21 % and 0.17 %, respectively. When we compare Fig. 5a and 5b, we see that the combination of F1 and F3 provides a much better discrimination of non-biological aerosol. However, there is a remaining interference of about 0.2 % from non-biological aerosol. According to our first experiment, which quantifies the fluorescence signal coming from ammonium sulphate aerosol, it can be accepted that all measured fluorescence is due to the soot aerosol. If we assume total aerosol number concentrations expected in a semi-rural area to be around $600\,l^{-1}$ (see the results presented in Sect. 3.2), combustion aerosol emissions might contribute to the detected fluorescent biological aerosol number concentration by about one particle l^{-1} at most.

ACPD
12, 17607–17656, 2012

After testing several non-biological and biological aerosol mixtures, we had the opportunity to make some test measurements by using different bacterial species, which had been prepared within the BIO-05 campaign for the purpose of investigating their ice nucleation capabilities in cloud chamber experiments. We present here only one example from the cloud expansion experiments which were done within the BIO-05 campaign. The following results clearly show the capability of WIBS-4 in the detection of bacterial species. Because we did not use classical bacterial growing methods to check the viability status of the used bacterial strains we can only speculate about the viable and non-viable bacteria number concentration during these experiment. Assuming that channel F1 measures only the fluorescence from tryptophan (which is an indicator for biological organisms) and the channel F3 from NADH (which is an indicator for living biological organisms), we can speculate that the combination of F1 and F3 (FBAP) gives the fraction of viable species. The lower plots in Fig. 6a, b show that (i) all bacterial species in the cloud chamber (AIDA) were counted based on the F1 channel and (ii) only a minor fraction of those particles were classified to be alive based on the FBAP combination. This would mean that only around 10 % of all bacterial cells managed to survive the harsh conditions during a cold cloud expansion experiment. Although this interpretation is quite speculative at the moment, the observation gives us the motivation for future studies. These studies will aim at the comparison of the WIBS4-based bacteria detection capabilities with classical techniques in order to see if the instrument can also reliably discriminate the fraction of viable bacterial cells.

As a conclusion of the above laboratory experiments we can say that the fluorescence signal from ammonium sulphate aerosol can be completely suppressed by using the combination of the F1 and F3 fluorescence channels. As a second important result of these experiments we can admit that there was a small but significant amount of fluorescence signal induced by mineral dust particles. This could be the first indicator of biological species residing on the surfaces of the dust particles. Another important finding is the low cross sensitivity of the used biological aerosol definition (FBAP: F1

ACPD
12, 17607–17656, 2012

and F3) in the case of CAST fossil fuel combustion aerosol, which is found to be only around 0.2 %.

3.2 Ambient measurements

We used the WIBS-4 to characterize the ambient aerosol in the vicinity of the IMK-AAF (Institute for Meteorology and Climate Research, Atmospheric Aerosol Research) building at KIT (Karlsruhe Institute of Technology, Campus North) in Karlsruhe, Germany (49° 5′ 43.58″ N, 8° 25′ 45.04″ E; 112 m a.s.l.). The WIBS-4 inlet was placed on the roof of the aerosol laboratory, i.e. approximately 5 m above the ground. We used a Total Suspended Particles inlet (TSP, Digitel, Model DTSP01/00/16) to sample ambient aerosol. The TSP inlet is an omnidirectional inlet, which is widely used for general particulate pollution monitoring. There are different versions available for both high volume and low volume air pollution monitoring applications. In our study, we used the low-volume TSP inlet that requires a sample flow rate of 1 $m^3 h^{-1}$ (16.67 $l min^{-1}$). With this sample flow rate the TSP inlet is specified to collect particles with a wide spectrum of sizes up to around 30–40 µm. The 13 mm inner diameter stainless steel sampling tube downstream the TSP inlet penetrates the roof of the laboratory where it is fitted to a 40 mm inner diameter flow tube, which is operated at flow rate of 16.67 $l min^{-1}$. At the far end of this tube another 13 mm inner diameter sampling tube penetrates the wider flow tube by about 40 cm forming an isokinetic sampling tube for WIBS-4, which has a sample flow rate of 2.5 $l min^{-1}$. The sampling is said to be isokinetic when it is isoaxial and the mean sample flow velocity through the face of the inlet is equal to the gas flow velocity (Baron et al., 2001). The final connection between WIBS-4 and the TSP isokinetic inlet system was made using an electrically conductive silicon rubber tube (length 35 cm, inner diameter 13 mm).

The measurement site is surrounded by a forest from the north-east to the south-west and has a distance from the closest highway of almost 550 m. Ambient temperature (T), relative humidity (RH) and pressure were simultaneously measured using a chilled mirror hygrometer. Wind speed and direction were measured by using a 3-D

ACPD
12, 17607–17656, 2012

sonic anemometer (USA-1, ACH+T, one s time resolution). We obtained additional wind data together with precipitation (mm) and global solar radiation ($W\,m^{-2}$) data from the meteorological tower of KIT located about 500 m to the south-west of the measurement site. WIBS-4 sampled the ambient air continuously over a period of 1 yr (1 April 2010–1 April 2011). The measurement stopped sometimes because of undefined problems with the data acquisition software. Those missing data periods are represented by gaps in the figures below.

As a consequence of the findings from the above laboratory tests, we used the combination of the two fluorescence channels F1 and F3 (FBAP) to discriminate biological from non-biological aerosol particles. Fifteen min averages of the FBAP number concentrations, the relative FPAB aerosol fractions and their size distributions are illustrated in Fig. 7. To highlight the seasonal variability of the atmospheric FBAP component, Fig. 7 is composed of 4 panels representing the spring (April–June), summer (July–September), autumn (October–December) and winter (January–March) periods.

Based on this one year data set, we can conclude that N_{FBAP} and N_T showed large variability (see Fig. 8 and Table 2). However, the FBAP number concentrations and number fractions exhibit a clear seasonal cycle. We observed high FBAP number concentrations and FBAP number fractions from late spring until early autumn. On the other hand, we found lowest FBAP number concentrations in the winter period. These results are also in a good agreement with the typical fungal spore releases in Europe (Winiwarter et al., 2009). Spring N_{FBAP} changed between 1.2–337 l^{-1} while the relative contribution of FBAP to the total aerosol particle (TAP) varied between 0.26–40 % (Fig. 7a). Summer N_{FBAP} and $N_{FBAP}\,N_T^{-1}$ were between 0.58–244 l^{-1} and between 0.90–42 %, respectively (Fig. 7b). Autumn N_{FBAP} and $N_{FBAP}\,N_T^{-1}$ varied between 0.29–135 l^{-1} and between 0.32–30 %, respectively (Fig. 7c). The ranges of FBAP number concentrations and $N_{FBAP}\,N_T^{-1}$ aerosol fractions were significantly reduced in the winter period to ranges of 0.29–80 l^{-1} and 0.43–18 %, respectively (Fig. 7d).

Figure 8 shows the statistical analysis of the fifteen min average number concentrations for the individual seasons. The corresponding values were also tabulated in

ACPD
12, 17607–17656, 2012

Table 2. As already mentioned, the statistical analysis of the data revealed that fluorescent biological aerosol number concentrations (N_{FBAP}) and the relative contribution of FBAP to TAP ($N_{FBAP}\,N_T^{-1}$) exhibited a clear seasonal dependence (Fig. 8b, c). On the other hand the seasonal mean of N_T (Fig. 8a) was almost constant over the course of our one year sampling period, which had the minimum value in autumn and the maximum value in spring. In contrast to the summer and autumn periods, the spring and winter N_T possessed strong fluctuations which are reflected in the length of the corresponding 10–90th percentile bars in Fig. 8a. We can speculate that these fluctuations are due to local sources (e.g. grass cutting events around the site). These fluctuations appeared also in the figures which show the diurnal change of N_T (Fig. 10).

We also analysed the diurnal changes in the FBAP and TAP number concentrations and distributions. Figure 9 represents these diurnal changes of FBAP for the different seasons. In spring term, N_{FBAP} started to increase after sunset and reached its maximum value in the early morning h (Fig. 9a). The lowest N_{FBAP} values were measured during day time, between 12:00 and 15:00. On the other hand, we observed a steep increase in N_T after sunrise and the maximum TAP number concentrations were observed during day time (Fig. 10a). After 15:00, N_T started to decrease until sunset. After the sunset, N_T slightly increased and stayed constant until the next sunrise. In spring, we observed a diel mode at ~2.5 µm for FBAP. In summer, we again observed clear diurnal changes in FBAP and TAP number concentrations. N_{FBAP} was, like in spring term, high between 18:00 and 09:00 (Fig. 9b). Besides, the decrease in the N_{FBAP} shifted to early noon h. Similar to the spring term, N_T was high during day time and lower but almost constant between 17:00 and 06:00. A steep increase in N_T was again observed after sunrise until 12:00 and it started to decrease again after 12:00. We observed the same diel mode at ~2.5 µm which suggests the release of a specific type of biological aerosol around the measurement site. The observed diurnal changes in TAP number concentrations with larger concentrations of bigger particles during day time suggest that the reported diurnal changes of the N_{FBAP} concentrations is not simply due to convective mixing and dilution during day time (Garland et al., 2008, 2009) but

ACPD
12, 17607–17656, 2012

indicates a specific release mechanism. This specific release mechanism is discussed in the next section in detail.

In the autumn period, we observed a similar diurnal change of FBAP in analogy to the spring term (Fig. 9c). The same diel mode around 2.5 µm was again observed. On the other hand, N_T stayed constant during the whole day. However, in contrast to the spring term, autumn and summer biological aerosol size showed a broader distribution. A higher number concentration of larger particles was observed, which may reflect another type of aerosol release in this time period, i.e. different kind of fungal spore or pollen release. Since this type of aerosol consists of larger particles (here >16 µm), they saturate the detector and fall to the last size bin of the WIBS-4 (greenish solid line on lower panels of Fig. 9b–d). Unlike the other three seasons, in winter we observed almost constant number concentrations of FBAP and TAP (Figs. 9d and 10d). Night time N_T values, however, were for the first time higher than during day time. N_T started to increase after 17:00, reached its maximum value at 23:00 and started to decrease after 04:00. Again a diel mode of FBAP at 2.5 µm was observed. However, this mode was not as clear as it was in other three seasons.

Figure 11 shows the fluorescence data combined with asymmetry factor data for FBAP and TAP. It can be clearly seen that the observed FBAP diel mode consists of less spherical particles having AF values between 10 and 40, while TAP includes another type of aerosol which is more spherical (AF smaller than 10).

As a result of this diurnal analysis, we can give the following conclusions. First, we observed one distinct mode for FBAP at ~2.5 µm and with a specific particle shape, which indicates the emission of a site specific biological aerosol type (most likely spores). Second, the diurnal change in N_T with strong fluctuations during day time may be explained by the boundary layer mixing effects and local sources. Diurnal changes of TAP in the spring period suggest that local events can significantly influence the coarse mode ($D_p > 2.5$ µm, optical size) aerosol distribution and should be carefully considered to prevent any over estimation of biological and non-biological aerosol. However, the diurnal changes of FBAPs were considerably different from the

ACPD
12, 17607–17656, 2012

change in N_T which suggests that FBAP sources appear to have a specific release mechanism with a strong diurnal cycle.

3.2.1 Correlation of FBAP with meteorological data

Figures 12, 13, 14 and 15 show the fluorescence data combined with several meteorological data for four selected sampling periods. Because the fluorescence data showed certain diurnal patterns, we looked for correlations of the FBAP number concentration with different meteorological parameters. To get a first overview of the role of each meteorological parameter for this correlation, we plotted all data in the same figure. In Figs. 12 and 13 the strong correlation between N_{FBAP} and the relative humidity is eye-catching, especially during clear sky periods (indicated by distinct diurnal courses of the global solar radiation) with warm and dry days and cool and humid nights (i.e. between 22 May–25 May). For these periods we observed a continuous release of biological aerosol particles during night time which is obviously triggered by the highly humid conditions. This kind of biological aerosol release was investigated by several groups in the literature. For instance, Hirst (1953) found a direct relation between *Basidiomycota* (BMC) type of fungal spore release and relative humidity. This type of fungus ejects its spores according to an active mechanism and the ambient relative humidity is the key factor (Pringle et al., 2005; Elbert et al., 2007).

We performed a statistical analysis of the data to quantify the correlation between the FBAP number concentration and the relative humidity. Mean and median FBAP number concentration values were compared with the relative humidity values, which were measured at the same time, and FBAP numbers falling into 1 % relative humidity bins were calculated. The resulting curves were then fitted according to a power law function. The coefficients of determination (R^2) for the non-linear regressions were also calculated and reported. Figure 16 represents the correlation between N_{FBAP} and relative humidity for the four seasons. This figure clearly shows that the FBAP number concentration increased exponentially for relative humidity conditions higher than about 75 % until 98 %. Our finding is in a good agreement with the results published

ACPD
12, 17607–17656, 2012

by Gabey et al. (2010). As a conclusion of this correlation, we can also speculate that our results are consistent with the well-known behaviour of *Basidiomycota* (BMC) type of fungal spores, which are released mostly during night time and under humid conditions. However, under the light of our findings it is not possible to come to a conclusion about the spore type and the exact release mechanism of these particles.

Fröhlich-Nowoisky (2012) presented the DNA-based analysis of airborne fungi in continental, coastal and marine air. They concluded that the BMC dominate continental air, while *Ascomycota* (AMC) prevails mostly in marine and coastal air. They also showed that most of the BMC species detected in continental, coastal and marine air belong to a single taxonomic class, the *Agaricomycetes*. A clear identification of this kind of spore release would be possible by collecting filter samples and analysing these samples with electron microscopy and DNA-based techniques in order to specify the spore type. The Polymerase Chain Reaction (PCR) method for instance makes it possible to identify specific types of fungal species (Alvarez, 1995; Zhou et al., 2000; Nowoisky et al., 2009; Fröhlich-Nowoisky et al., 2012; Lang-Yona et al., 2012). This will be performed in follow-up studies, but is beyond the scope of this work. On the other hand, we did not find any evidence of passive bioaerosol release, which is generally related to the wind speed and wind direction or precipitation. However, in some cases slightly increased FBAP number concentrations were observed following rain events.

3.2.2 Size dependence of the FBAP/TAP ratio

Another valuable result of this study is quantifying the size dependence of the relative contribution of FBAP to TAP. Figure 17 illustrates the relative contribution of FBAP number concentration to TAP for four sampling terms. By following the study published by Huffman et al. (2010), we integrated our data as 20 min time intervals, which corresponds to a total air volume of ~5 l. By following the statistical calculation used by Huffman et al. (2010), we assumed that WIBS-4 should be able to detect at least one biological particle in 5 l of sampled air. Huffman et al. (2010) reported the number ratio of FBAP to TAP to be less than 10 % for the fine particulate matter (1.0 µm <

ACPD
12, 17607–17656, 2012

Da < 2.5 µm, aerodynamic size) in Mainz, Germany. For the same seasonal period and including almost the same size range, WIBS-4 measured about 20 % contribution (Fig. 17c). Overlapping of the median and the mean curves on this ratio plots asserts the good counting statistics of the instrument. A deviation from this overlapping could be because of the low counting statistics, which is reflected on median curves for bigger particles.

In the spring period, we observed one broadened peak around 3 µm (Fig. 17a) which is reflected by both median and the mean ratio curves. For the coarse mode particles the median ratio curve dropped gradually after this peak, while the mean ratio curve increased for the bigger particles. The decrease on the median ratio curve in this period can be explained also by low counting statistics, which forces the median towards zero. $N_{\mathrm{FBAP}}\,N_{\mathrm{T}}^{-1}$ was calculated as ∼30 % for the fine particles ($D_{\mathrm{p}} < 2.5$ µm, optical size) in this season. Median and mean ratio curves differed for particle sizes larger than ∼3 µm, which shows that during spring term the FBAP population was dominated by small particles. In the summer period, the median ratio curve shows a different behaviour compared to the spring period (Fig. 17b), whereas the mean ratio curve has preserved almost the same trend. The median ratio curve maximum position is shifted to slightly larger sizes and, therefore, the counting statistics was obviously better for larger particles compared to the spring period. The $N_{\mathrm{FBAP}}\,N_{\mathrm{T}}^{-1}$ (%) was calculated as ∼30 % for fine mode particles and ∼40 % for the coarse mode particles. During the autumn period (Fig. 17c), a similar pattern was observed with a small shift of the median curve maximum. $N_{\mathrm{FBAP}}\,N_{\mathrm{T}}^{-1}$ (%) was found to be around 20 % for fine particles and between 30–40 % for coarse mode particles. These observations show that the coarse mode of the FBAP population was significantly increased in the summer and autumn seasons compared to the spring, which indicates the release of additional larger bioarosol particles (e.g. spores and pollens) in these periods. It can clearly be seen that during the winter season (Fig. 17d), the relative contribution of FBAP to TAP was decreased to around 15 % for fine particles which represents the lowest background

ACPD
12, 17607–17656, 2012

FBAP concentration present during all year. However, the coarse mode FBAP contribution was between 20–50 % and, thus, comparable to the other seasons.

4 Conclusions and outlook

In this paper, we presented several laboratory tests and a one-year online measurement of ambient aerosol by using the UV-LIF method, in a semi-urban area at Karlsruhe Institute of Technology (KIT), Campus North, Germany. For this purpose, a recently developed single particle bioaerosol sensor (WIBS mk4) was used. To our knowledge, this study is the first long term usage of WIBS in a field campaign which provides insight into the capabilities of this instrument for analysing the seasonal variations of Fluorescent Biological Aerosol Particles (FBAP) in the atmospheric aerosol. Laboratory measurements supported and clarified the accuracy of defined threshold to discriminate the biological from non-biological aerosols. As a final conclusion of these laboratory tests we can indicate that, although there are particles which fluoresce and interfere in this method, the use of the combination of two fluorescence channels provides a good discrimination of biological aerosol. For example, ammonium sulphate aerosol which prevails in the ambient air can be easily differentiated by this method. Furthermore, it is also possible to distinguish mineral dust which represents an important component of the atmospheric aerosol that affects atmospheric processes in several ways, can also be separated from fluorescent biological aerosol particles. A low cross sensitivity of the used biological aerosol definition (FBAP: F1 and F3) in the case of CAST soot aerosol was also observed. However, the contribution was only around 0.2 %. In future studies, other measurement parameters like the particle asymmetry factor can be exploited to provide an even better discrimination of biological aerosol.

FBAP were observed during the entire sampling period. FBAP number concentrations increased gradually from spring to summer and decreased in the same manner towards the end of autumn and reached a minimum value in winter. Fluorescent biological aerosol particle number concentration was between 10–53 l^{-1} (mean = 29 l^{-1})

ACPD
12, 17607–17656, 2012

and 20–80 l^{-1} (mean = 46 l^{-1}) in spring and summer, respectively. In autumn and winter, N_{FBAP} was between 8–54 l^{-1} (mean = 29 l^{-1}) and 8–32 l^{-1} (mean = 31 l^{-1}), respectively. In spring and summer, the relative contribution of FBAP to the total aerosol particle (TAP) varied between 0.26–40 % (mean = 7 %) and 0.90–42 % (mean = 11 %) while in autumn and winter the ratio varied between 0.32–30 % (mean = 7 %) and 0.43–18 % (mean = 4 %), respectively.

The correlation of the WIBS fluorescence measurements with meteorological data showed a strong relation of the FBAP number concentrations with the relative humidity. Measured wind data was also presented on the same plot (Fig. 12). However, FBAP concentrations changed independently of the wind speed and the wind direction. In most of the time, FBAP was dominated by one distinct mode of particles which appeared between 2 to 3 µm and which we attribute to a site-specific spore type. Although a detailed speciation is not possible with the UV-LIF method, the fact that this FBAP mode shows a strong correlation with the relative humidity, which reveals an effective release mechanism during humid clear-sky nights, points toward a *Basidiomycota* type of fungal spore.

All published studies about the rapid detection of primary biological aerosol particles using the UV-LIF method were limited because of the well-known interference from non-biological fluorescent aerosol which is a certain amount of the total aerosol. To our knowledge, this is the first study which combines laboratory experiments with long term field studies in order to quantify these possible interferences. The presented results motivate us to conduct further long term field measurements at different locations using the WIBS-4 instrument. Nevertheless, we need a better understanding of how biological particles control their fluorescence ability under different conditions like mechanical stress and heat, humidity, aging, etc. Including all these parameters new laboratory experiments need to be designed and different relevant biological and non-biological aerosol samples should be investigated. In this way and exploiting the additional information from the shape sensitive detector of WIBS-4 it should be possible

ACPD
12, 17607–17656, 2012

to define a robust discrimination method which provides a better discrimination of biological ambient aerosol under different atmospheric conditions.

Acknowledgements. This work was funded by the Graduate School for Climate and Environment (GRACE) at KIT and the Helmholtz-Gemeinschaft Deutscher Forschungszentren as part of the program "Atmosphere and Climate". The authors thank Corinna Hoose for the fruitful discussions and her review of the manuscript. We gratefully acknowledge support by Paul H. Kaye and his team at University of Hertfordshire for building WIBS-4 instrument and their outstanding support. Thanks are dedicated to Claudia Linke, Olga Dombrowski, Georg Scheurig, and Rainer Buschbacher for their support during the laboratory tests. Andy Gabey is thanked for providing us with his Matlab analysis program and for his support to adapt it to WIBS-4. We thank Martin Kohler for the data from the meteorological tower. We acknowledge support by Deutsche Forschungsgemeinschaft and Open Access Publishing Fund of Karlsruhe Institute of Technology.

The service charges for this open access publication have been covered by a Research Centre of the Helmholtz Association.

References

Alvarez, A. J., Buttner, M. P., and Stetzenbach, L. D.: PCR for bioaerosol monitoring: sensitivity and environmental interference, Appl. Environ. Microb., 61, 3639–3644, 1995.

Bauer, H., Kasper-Giebl, A., Loflund, M., Giebl, H., Hitzenberger, R., Zibuschka, F., and Puxbaum, H.: The contribution of bacteria and fungal spores to the organic carbon content of cloud water, precipitation and aerosols, Atmos. Res., 64, 109–119, 2002.

Bauer, H., Claeys, M., Vermeylen, R., Schueller, E., Weinke, G., Berger, A., and Puxbaum, H.: Arabitol and mannitol as tracers for the quantification of airborne fungal spores, Atmos. Environ., 42, 588–593, doi:10.1016/j.atmosenv.2007.10.013, 2008.

Brosseau, L. M., Vesley, D., Rice, N., Goodell, K., Nellis, M., and Hairston, P.: Differences in detected fluorescence among several bacterial species measured with a direct-reading particle sizer and fluorescence detector, Aerosol Sci. Tech., 32, 545–558, 2000.

ACPD

12, 17607–17656, 2012

Burrows, S. M., Butler, T., Jöckel, P., Tost, H., Kerkweg, A., Pöschl, U., and Lawrence, M. G.: Bacteria in the global atmosphere – Part 2: Modeling of emissions and transport between different ecosystems, Atmos. Chem. Phys., 9, 9281–9297, doi:10.5194/acp-9-9281-2009, 2009.

Christner, B. C., Morris, C. E., Foreman, C. M., Cai, R., and Sands, D. C.: Ubiquity of biological ice nucleators in snowfall, Science, 319, 1214, doi:10.1126/science.1149757, 2008.

Cooke, W. F., Liousse, C., Cachier, H., and Feichter, J.: Construction of a 1 degrees x 1 degrees fossil fuel emission data set for carbonaceous aerosol and implementation and radiative impact in the ECHAM4 model, J. Geophys. Res.-Atmos., 104, 22137–22162, 1999.

Crawford, C., Reponen, T., Lee, T., Iossifova, Y., Levin, L., Adhikari, A., and Grinshpun, S. A.: Temporal and spatial variation of indoor and outdoor airborne fungal spores, pollen, and (1→3)-β-d-glucan, Aerobiologia, 25, 147–158, doi:10.1007/s10453-009-9120-z, 2009.

De Antoni Zoppas, B. C., Valencia-Barrera, R. M., Vergamini Duso, S. M., and Fernández-González, D.: Fungal spores prevalent in the aerosol of the city of Caxias do Sul, Rio Grande do Sul, Brazil, over a 2-year period (2001–2002), Aerobiologia, 22, 117–124, doi:10.1007/s10453-006-9022-2, 2006.

Despres, V. R., Huffman, J. A., Burrows, S. M., Hoose, C., Safatov, A. S., Buryak, G., Fröhlich-Nawoisky, J., Elbert, W., Andreae, M. O., Pöschl, U., and Jaenicke, R.: Primary biological aerosol particles in the atmosphere: a review, Tellus B, doi:10.3402/tellusb.v64i0.15598, 2012.

Diehl, K., Quick, C., Matthias-Maser, S., Mitra, S. K., and Jaenicke, R.: The ice nucleating ability of pollen – Part I: Laboratory studies in deposition and condensation freezing modes, Atmos. Res., 58, 75–87, 2001.

Diehl, K., Matthias-Maser, S., Jaenicke, R., and Mitra, S. K.: The ice nucleating ability of pollen – Part II: Laboratory studies in immersion and contact freezing modes, Atmos. Res., 61, 125–133, 2002.

Elbert, W., Taylor, P. E., Andreae, M. O., and Pöschl, U.: Contribution of fungi to primary biogenic aerosols in the atmosphere: wet and dry discharged spores, carbohydrates, and inorganic ions, Atmos. Chem. Phys., 7, 4569–4588, doi:10.5194/acp-7-4569-2007, 2007.

Eversole, J. D., Cary, W. K., Scotto, C. S., Pierson, R., Spence, M., and Campillo, A. J.: Continuous bioaerosol monitoring using UV excitation fluorescence: outdoor test results, Field Anal. Chem. Tech., 5, 205–212, 2001.

ACPD
12, 17607–17656, 2012

Foot, V. E., Kaye, P. H., Stanley, W. R., Barrington, S. J., Gallagher, M., and Gabey, A.: Lowcost real-time multiparameter bio-aerosol sensors, Proc. SPIE Conference on Optically Based Biological and Chemical Sensing, Cardiff, Wales, UK, 71160I-71112, 2008.

Fröhlich-Nowoisky, J., Burrows, S. M., Xie, Z., Engling, G., Solomon, P. A., Fraser, M. P., Mayol-Bracero, O. L., Artaxo, P., Begerow, D., Conrad, R., Andreae, M. O., Després, V. R., and Pöschl, U.: Biogeography in the air: fungal diversity over land and oceans, Biogeosciences, 9, 1125–1136, doi:10.5194/bg-9-1125-2012, 2012.

Gabey, A. M., Gallagher, M. W., Whitehead, J., Dorsey, J. R., Kaye, P. H., and Stanley, W. R.: Measurements and comparison of primary biological aerosol above and below a tropical forest canopy using a dual channel fluorescence spectrometer, Atmos. Chem. Phys., 10, 4453–4466, doi:10.5194/acp-10-4453-2010, 2010.

Gabey, A. M., Stanley, W. R., Gallagher, M. W., and Kaye, P. H.: The fluorescence properties of aerosol larger than 0.8 µm in urban and tropical rainforest locations, Atmos. Chem. Phys., 11, 5491–5504, doi:10.5194/acp-11-5491-2011, 2011.

Garland, R. M., Yang, H., Schmid, O., Rose, D., Nowak, A., Achtert, P., Wiedensohler, A., Takegawa, N., Kita, K., Miyazaki, Y., Kondo, Y., Hu, M., Shao, M., Zeng, L. M., Zhang, Y. H., Andreae, M. O., and Pöschl, U.: Aerosol optical properties in a rural environment near the mega-city Guangzhou, China: implications for regional air pollution, radiative forcing and remote sensing, Atmos. Chem. Phys., 8, 5161–5186, doi:10.5194/acp-8-5161-2008, 2008.

Garland, R. M., Schmid, O., Nowak, A., Achtert, P., Wiedensohler, A., Gunthe, S. S., Takegawa, N., Kita, K., Kondo, Y., Hu, M., Shao, M., Zeng, L. M., Zhu, T., Andreae, M. O., and Pöschl, U.: Aerosol optical properties observed during campaign of air quality research in Beijing 2006 (CAREBeijing-2006): characteristic differences between the inflow and outflow of Beijing city air, J. Geophys. Res.-Atmos., 114, D00G04, doi:10.1029/2008jd010780, 2009.

Gilbert, G. S.: Nocturnal fungi: airborne spores in the canopy and understory of a Tropical Rain Forest, Biotropica, 37, 462–464, 2005.

Gregory, P. H. and Hirst, J. M.: The summer air-spora at Rothamsted in 1952, J. Gen. Microbiol., 17, 135–152, 1957.

Gruber, S., Matthias-Maser, S., and Jaenicke, R.: Concentration and chemical composition of aerosol particles in marine and continental air, J. Aerosol Sci., 30, 9–10, 1999.

ACPD
12, 17607–17656, 2012

Hairston, P. P., Ho, J., and Quant, F. R.: Design of an instrument for real-time detection of bioaerosols using simultaneous measurement of particle aerodynamic size and intrinsic fluorescence, J. Aerosol Sci., 28, 471–482, 1997.
Hallar, A. G., Chirokova, G., McCubbin, I., Painter, T. H., Wiedinmyer, C., Dodson, C.: Atmospheric bioaerosols transported via dust storms in the Western United States, Geo. Res. Lett., 38, L17801, doi:10.1029/2011GL048166, 2011.
Hirst, E., Kaye, P. H., Greenaway, R. S., Field, P., and Johnson, D. W.: Discrimination of micrometre-sized ice and super-cooled droplets in mixed-phase cloud, Atmos. Environ., 35, 33–47, 2001.
Hirst, J. M.: Changes in atmospheric spore content: diurnal periodicity and the effects of weather, Trans. Brit. Mycol. Soc., 36, 375–393, 1953.
Ho, J.: Future of biological aerosol detection, Anal. Chim. Acta, 457, 125–148, 2002.
Huffman, J. A., Treutlein, B., and Pöschl, U.: Fluorescent biological aerosol particle concentrations and size distributions measured with an Ultraviolet Aerodynamic Particle Sizer (UV-APS) in Central Europe, Atmos. Chem. Phys., 10, 3215–3233, doi:10.5194/acp-10-3215-2010, 2010.
Jaenicke, R.: Abundance of cellular material and proteins in the atmosphere, Science, 308, p. 73, doi:10.1126/science.1106335, 2005.
Jaenicke, R., Matthias-Maser, S., and Gruber, S.: Omnipresence of biological material in the atmosphere, Environ. Chem., 4, 217–220, doi:10.1071/en07021, 2007.
Kaye, P. H., Stanley, W. R., Hirst, E., Foot, E. V., Baxter, K. L., and Barrington, S. J.: Single particle multichannel bio-aerosol fluorescence sensor, Opt. Express, 13, 3583–3593, 2005.
Kaye, P. H., Aptowicz, K., Chang, R. K., Foot, V., and Videen, G.: Angularly resolved elastic scattering from airborne particles – Potential for characterizing, classifying, and identifying individual aerosol particles, Opt. Biol. Part., 238, 31–61, 2007.
Lang-Yona, N., Dannemiller, K., Yamamoto, N., Burshtein, N., Peccia, J., Yarden, O., and Rudich, Y.: Annual distribution of allergenic fungal spores in atmospheric particulate matter in the Eastern Mediterranean; a comparative study between ergosterol and quantitative PCR analysis, Atmos. Chem. Phys., 12, 2681–2690, doi:10.5194/acp-12-2681-2012, 2012.
Matthias-Maser, S. and Jaenicke, R.: The size distribution of primary biological aerosol particles with radii > 0.2 µm in an urban/rural influenced region, Atmos. Res., 39, 279–286, 1995.
Matthias-Maser, S., Peters, K., and Jaenicke, R.: Seasonal variation of primary biological aerosol particles, J. Aerosol Sci., 26, 545–546, 1995.

ACPD
12, 17607–17656, 2012

Matthias-Maser, S., Reichert, K., and Jaenicke, R.: Primary biological aerosol particles at the high alpine site of Jungfraujoch/Switzerland, J. Aerosol Sci., 31, Suppl. 1, 955–956, 2000.
Monks, P. S., Granier, C., Fuzzi, S., Stohl, A., Williams, M. L., Akimoto, H., Amann, M., Baklanov, A., Baltensperger, U., Bey, I., Blake, N., Blake, R. S., Carslaw, K., Cooper, O. R., Dentener, F., Fowler, D., Fragkou, E., Frost, G. J., Generoso, S., Ginoux, P., Grewe, V., Guenther, A., Hansson, H. C., Henne, S., Hjorth, J., Hofzumahaus, A., Huntrieser, H., Isaksen, I. S. A., Jenkin, M. E., Kaiser, J., Kanakidou, M., Klimont, Z., Kulmala, M., Laj, P., Lawrence, M. G., Lee, J. D., Liousse, C., Maione, M., McFiggans, G., Metzger, A., Mieville, A., Moussiopoulos, N., Orlando, J. J., O'Dowd, C. D., Palmer, P. I., Parrish, D. D., Petzold, A., Platt, U., Pöschl, U., Prévôt, A. S. H., Reeves, C. E., Reimann, S., Rudich, Y., Sellegri, K., Steinbrecher, R., Simpson, D., ten Brink, H., Theloke, J., van der Werf, G. R., Vautard, R., Vestreng, V., Vlachokostas, C., and von Glasow, R.: Atmospheric composition change – global and regional air quality, Atmos. Environ., 43, 5268–5350, doi:10.1016/j.atmosenv.2009.08.021, 2009.
Möhler, O., Field, P. R., Connolly, P., Benz, S., Saathoff, H., Schnaiter, M., Wagner, R., Cotton, R., Krämer, M., Mangold, A., and Heymsfield, A. J.: Efficiency of the deposition mode ice nucleation on mineral dust particles, Atmos. Chem. Phys., 6, 3007-3021, doi:10.5194/acp-6-3007-2006, 2006.
Pan, Y.-L., Pinnick, R. G., Hill, S. C., Rosen, J. M., and Chang, R. K.: Single-particle laser-induced-fluorescence spectra of biological and other organic-carbon aerosols in the atmosphere: measurements at New Haven, Connecticut, and Las Cruces, New Mexico, J. Geophys. Res., 112, D24S19, doi:10.1029/2007jd008741, 2007.
Pinnick, R. G., Hill, S. C., Nachman, P., Pendleton, J. D., Fernandez, G. L., Mayo, M. W., and Bruno, J. G.: Fluorescence particle counter for detecting Airborne Bacteria and other biological particles, Aerosol Sci. Tech., 23, 653–664, doi:10.1080/02786829508965345, 1995.
Pöhlker, C., Huffman, J. A., and Pöschl, U.: Autofluorescence of atmospheric bioaerosols – fluorescent biomolecules and potential interferences, Atmos. Meas. Tech., 5, 37–71, doi:10.5194/amt-5-37-2012, 2012.
Pringle, A., Patek, S. N., Fischer, M., Stolze, J., and Money, N. P.: The captured launch of a ballistospore, Mycologia, 97, 866–871, 2005.
Rosenfeld, D., Lohmann, U., Raga, G. B., O'Dowd, C. D., Kulmala, M., Fuzzi, S., Reissell, A., and Andreae, M. O.: Flood or drought: how do aerosols affect precipitation?, Science, 321, 1309–1313, doi:10.1126/science.1160606, 2008.

ACPD
12, 17607–17656, 2012

Sánchez-Ochoa, A., Kasper-Giebl, A., Puxbaum, H., Gelencser, A., Legrand, M., and Pio, C.: Concentration of atmospheric cellulose: a proxy for plant debris across a west-east transect over Europe, J. Geophys. Res., 112, D23S08, doi:10.1029/2006jd008180, 2007.

Schauer, C., Niessner, R., and Poschl, U.: Analysis of nitrated polycyclic aromatic hydrocarbons by liquid chromatography with fluorescence and mass spectrometry detection: air particulate matter, soot, and reaction product studies, Anal. Bioanal. Chem., 378, 725–736, doi:10.1007/s00216-003-2449-1, 2004.

Schnaiter, M., Gimmler, M., Llamas, I., Linke, C., Jäger, C., and Mutschke, H.: Strong spectral dependence of light absorption by organic carbon particles formed by propane combustion, Atmos. Chem. Phys., 6, 2981–2990, doi:10.5194/acp-6-2981-2006, 2006.

Smith, D. J., Griffin, D. W., and Jaffe, D. A.: The high life: transport of microbes in the atmosphere, Eos. T. Am. Geophys. Un., 92, 249–256, 2011.

Stanley, W. R., Kaye, P. H., Foot, V. E., Barrington, S. J., Gallagher, M., and Gabey, A.: Continuous bioaerosol monitoring in a tropical environment using a UV fluorescence particle spectrometer, Atmos. Sci. Lett., 12, 195–199, doi:10.1002/asl.310, 2011.

Womiloju, T. O., Miller, J. D., Mayer, P. M., and Brook, J. R.: Methods to determine the biological composition of particulate matter collected from outdoor air, Atmos. Environ., 37, 4335–4344, doi:10.1016/s1352-2310(03)00577-6, 2003.

Wu, P. C., Tsai, J. C., Li, F. C., Lung, S. C., and Su, H. J.: Increased levels of ambient fungal spores in Taiwan are associated with dust events from China, Atmos. Environ., 38, 4879–4886, doi:10.1016/j.atmosenv.2004.05.039, 2004.

Yadav, R. K. P., Halley, J. M., Karamanoli, K., Constantinidou, H. I., and Vokou, D.: Bacterial populations on the leaves of Mediterranean plants: quantitative features and testing of distribution models, Environ. Exp. Bot., 52, 63–77, doi:10.1016/j.envexpbot.2004.01.004, 2004.

ACPD
12, 17607–17656, 2012

Table 1. Definition of abbreviations used in the text.

Short name	Description
TAP	Total aerosol particle (all particles measured by WIBS-4; fluorescent and non-fluorescent)
FBAP	Fluorescent biological aerosol particle (combination of F1 and F3)
N_T	Number of all particles measured by WIBS-4
N_{FBAP}	Number of fluorescent particles in F1 and F3
F1	Fluorescence detected in channel F1_280 (excitation at 280 nm, detection 310–400 nm)
F2	Fluorescence detected in channel F2_280 (excitation at 280 nm, detection 420–650 nm)
F3	Fluorescence detected in channel F2_370 (excitation at 370 nm, detection 420–650 nm)
F1 and F2	Particles showing fluorescence in channel F1_280 and F2_280
F2 and F3	Particles showing fluorescence in channel F2_280 and F2_370
F1 and F3	Particles showing fluorescence in channel F1_280 and F2_370
W_S	Wind speed
D_p	Optical particle size

ACPD
12, 17607–17656, 2012

Table 2. Integrated number concentrations for different measurement periods in the case of N_T and N_{FBAP} (0.8–16 µm): monthly and annual mean and median values between 1 April 2010 and 1 April 2011.

Quantity		Apr–Jun	Jul–Sep	Oct–Dec	Jan–Mar	One year
N_T (l^{-1})	Mean	691	520	468	633	583
	Median	474	465	392	510	461
N_{FBAP} (l^{-1})	Mean	29	46	29	19	31
	Median	24	40	23	17	25
N_{Non} (l^{-1})	Mean	545	354	310	426	416
	Median	338	287	234	354	300
$N_{FBAP}\,N_T^{-1}$ (%)	Mean	7.02	10.6	7.15	3.87	7.34
	Median	5.22	9.4	6.11	3.20	5.76

ACPD
12, 17607–17656, 2012

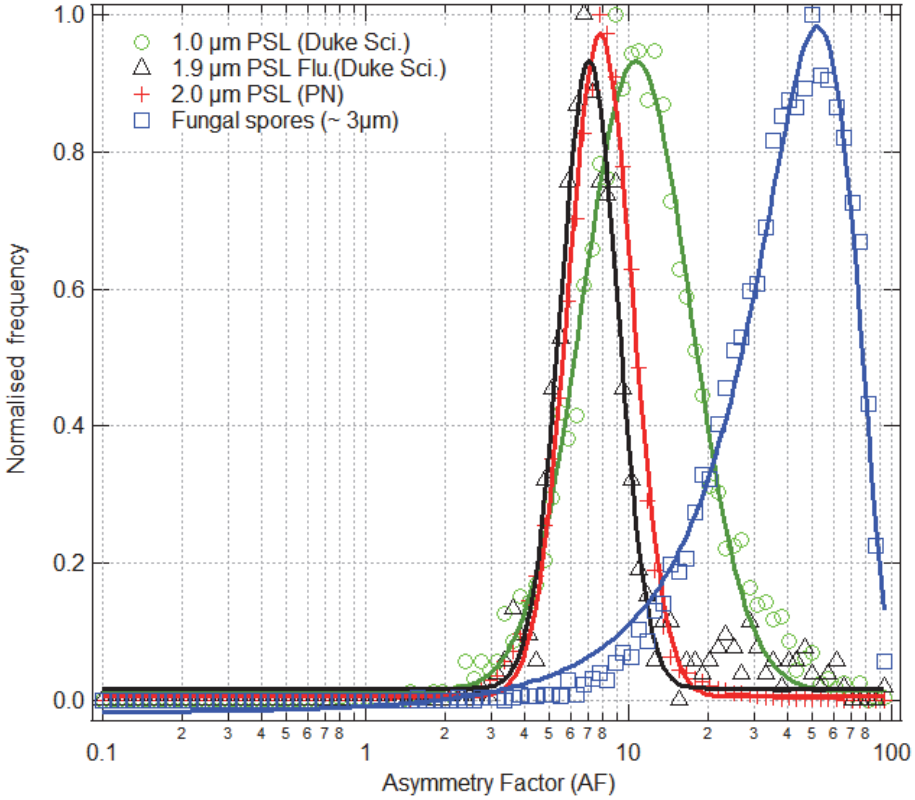

Fig. 1. Asymmetry Factor (AF) plot for PSL particles and *penicillium notatum* type of fungal spores.

ACPD
12, 17607–17656, 2012

Fluorescent biological aerosol particles (FBAPs)

E. Toprak and
M. Schnaiter

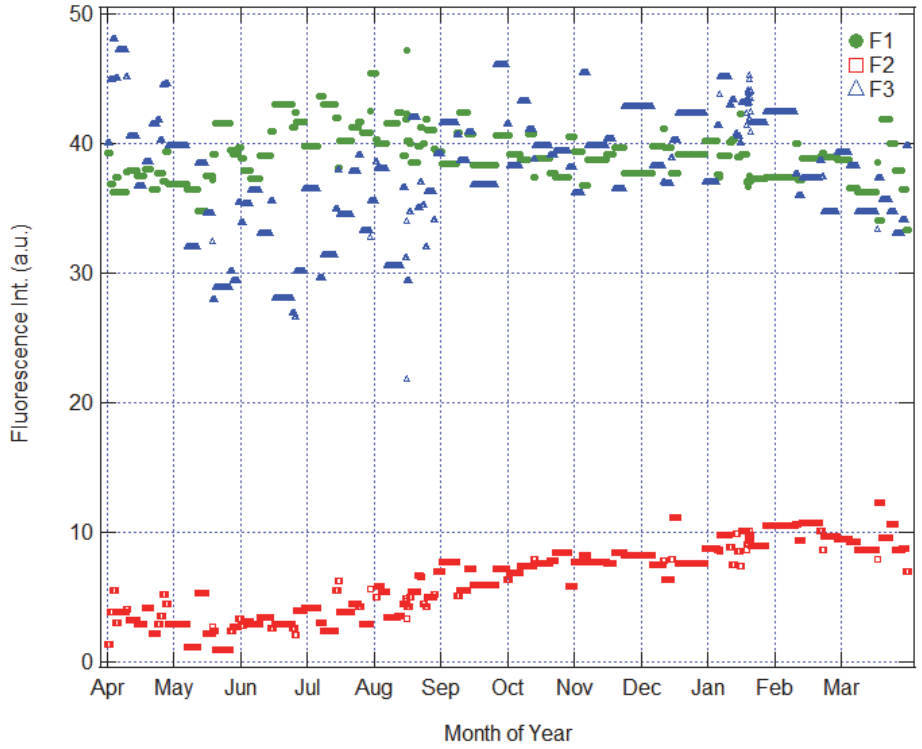

Fig. 2. Background fluorescence intensity change during a one year measurement period.

ACPD
12, 17607–17656, 2012

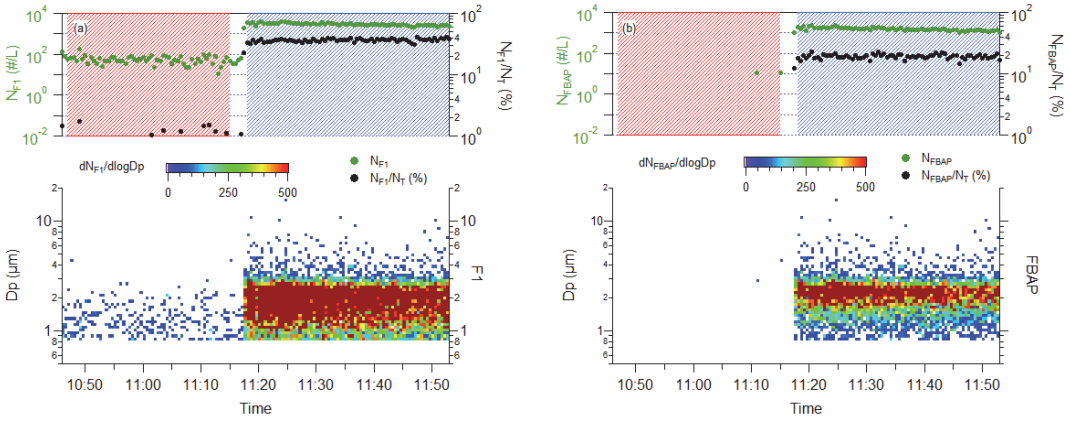

Fig. 3. WIBS-4 fluorescence data for ammonium sulphate aerosol and *penicillium notatum* spores measured during the BIO-05 campaign (24 March 2010 at IMK-AAF, KIT). Upper panel, left axis: number concentration of fluorescent biological aerosol particles in the size range 0.8–16 µm, green markers. Upper panel, right axis: ratio of the number of fluorescent particles to the total number concentration, black markers. Lower panel: size distribution ($dN/d\log D_p$) of fluorescent particles for the entire experiment period. The experiment period of pure ammonium sulphate aerosol is highlighted by a red shaded area while the mixture of ammonium sulphate and spores is represented by a blue shaded area. **(a)** shows the results using only events in channel F1 for discriminating biological particles while **(b)** uses the combination of simultaneous events in channels F1 and F3.

ACPD
12, 17607–17656, 2012

Fluorescent biological aerosol particles (FBAPs)

E. Toprak and M. Schnaiter

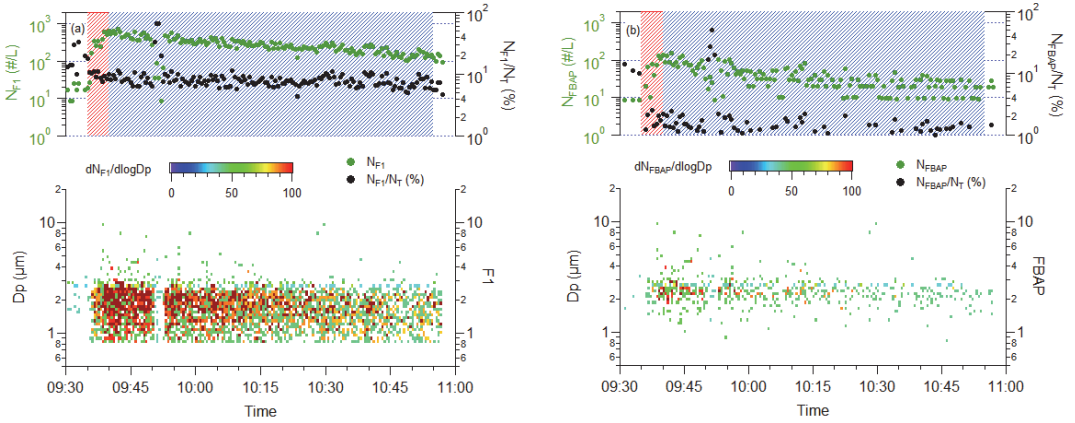

Fig. 4. WIBS-4 fluorescence data for a Saharan dust aerosol experiment conducted during BIO-05. The data are plotted in the same way as in Fig. 3. Red shaded area indicates the addition of Saharan dust aerosol into the chamber, while blue shaded area indicates the integrated sampling time.

ACPD
12, 17607–17656, 2012

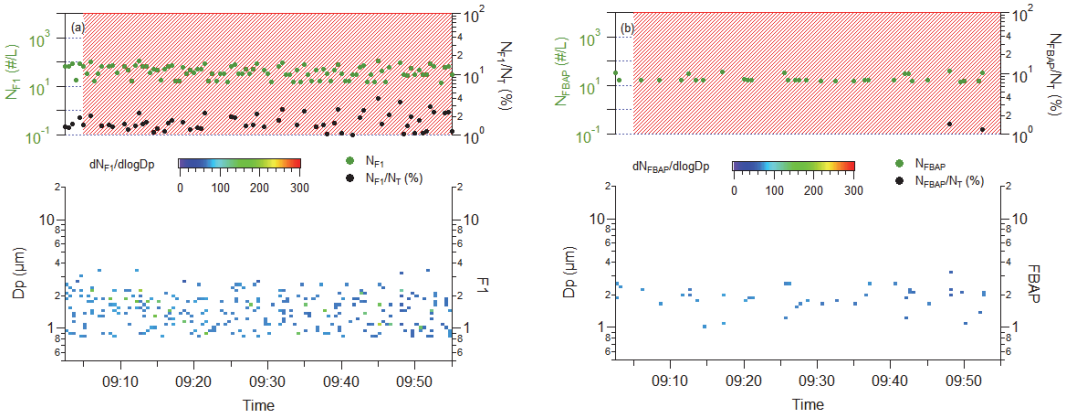

Fig. 5. WIBS-4 fluorescence data for ammonium sulphate – CAST soot aerosol mixture experiment conducted during BIO-05. The data are plotted in the same way as in Fig. 3. Pre-experimental period illustrated by a colorless area, while ammonium sulphate – CAST soot aerosol mixture is represented by a red shaded area.

ACPD
12, 17607–17656, 2012

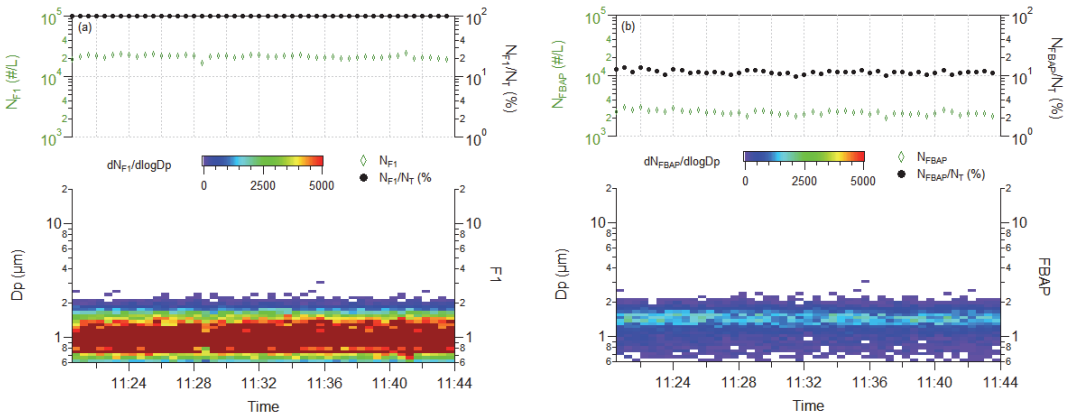

Fig. 6. WIBS-4 fluorescence data for *Pseudomonas syringae* type of bacterium isolated from cloud water type of bacteria experiment conducted during BIO-05. The data are plotted in the same way as in Fig. 3.

ACPD
12, 17607–17656, 2012

Fluorescent biological aerosol particles (FBAPs)

E. Toprak and M. Schnaiter

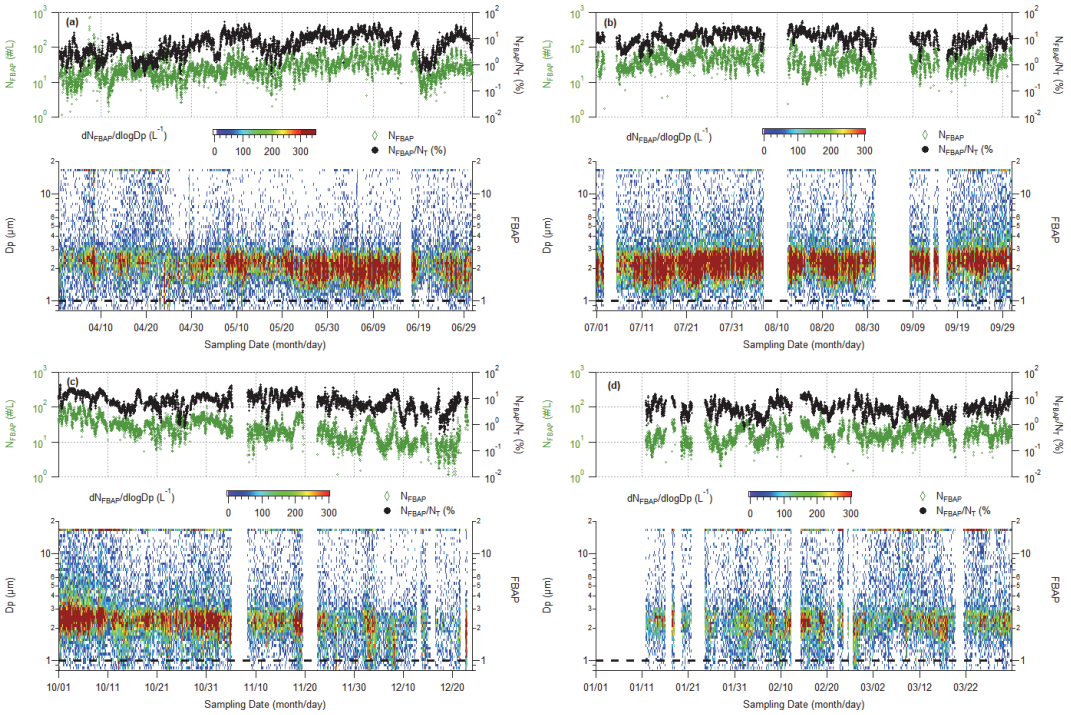

Fig. 7. WIBS-4 fluorescence data for one year online measurement term (April 2010–March 2011). The data are plotted in the same way as in Fig. 3. The colour scale in the lower image plots represents $dN_{FBAP}/d\log D_p$. **(a)** spring, **(b)** summer, **(c)** autumn, and **(d)** winter period.

ACPD
12, 17607–17656, 2012

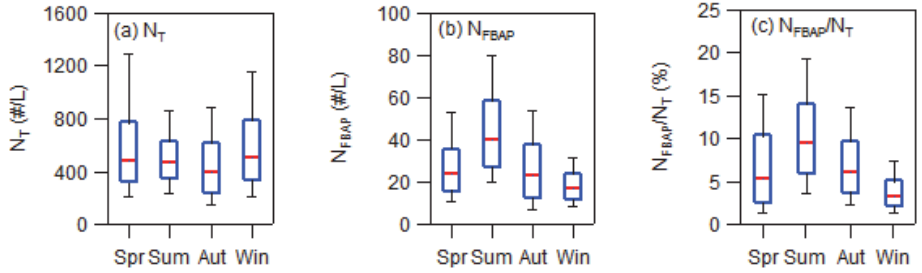

Fig. 8. Statistical representation of FBAP number concentrations and $N_{FBAP}N_T^{-1}$ for different seasons as box-and-whisker plots. Red solid line represents median (50th percentile), lower and upper limits of blue box show 25th and 75th percentiles, respectively. The black error bars show 10th and 90th percentiles.

ACPD
12, 17607–17656, 2012

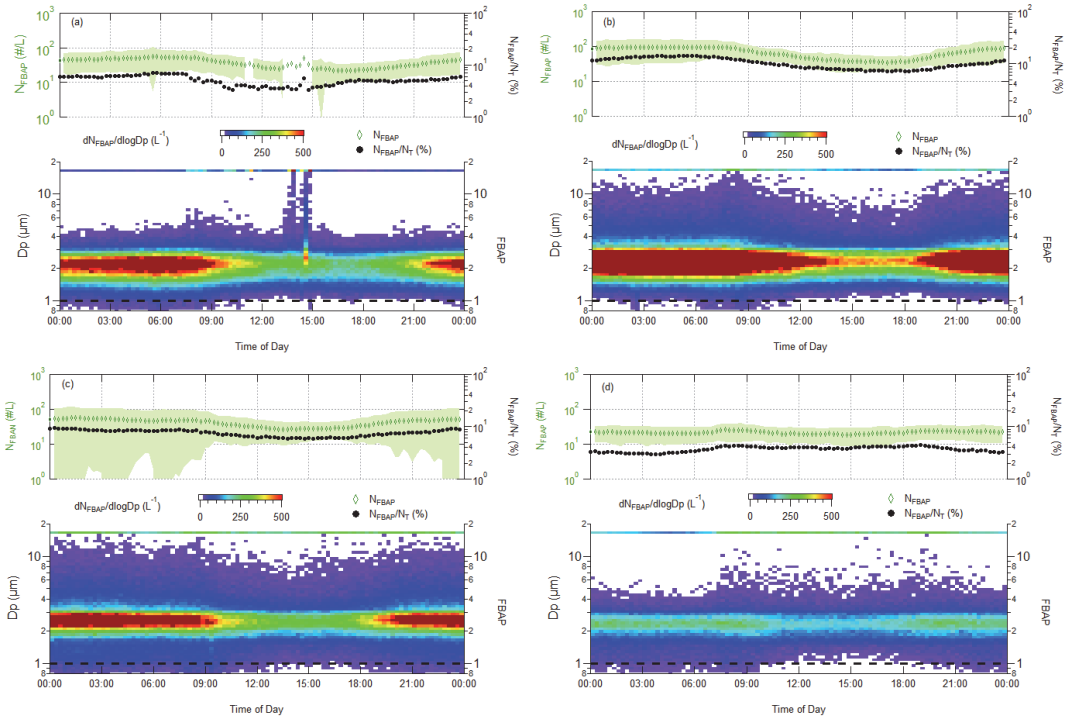

Fig. 9. WIBS-4 fluorescence data to show the diurnal changes of FBAP number concentrations and distribution for different sampling terms. The data were plotted in the same way as in Fig. 3. **(a)** spring, **(b)** summer, **(c)** autumn, **(d)** winter.

ACPD
12, 17607–17656, 2012

Fluorescent biological aerosol particles (FBAPs)

E. Toprak and M. Schnaiter

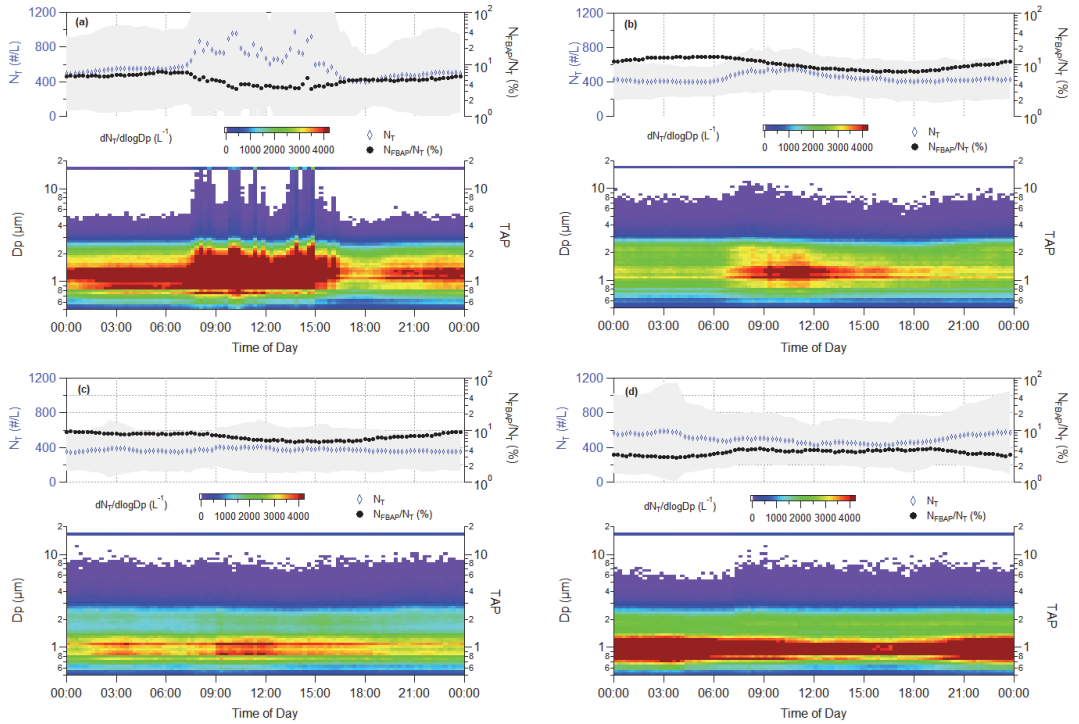

Fig. 10. Diurnal change of TAP number concentrations (upper panel) and size distributions (lower panel) for each measurement period (plots analogous to Fig. 9): **(a)** Spring, **(b)** Summer, **(c)** Autumn, and **(d)** Winter. Light-gray shaded area shows TAP concentration variability as the area between 25th–75th percentile traces.

ACPD
12, 17607–17656, 2012

Fluorescent biological aerosol particles (FBAPs)

E. Toprak and M. Schnaiter

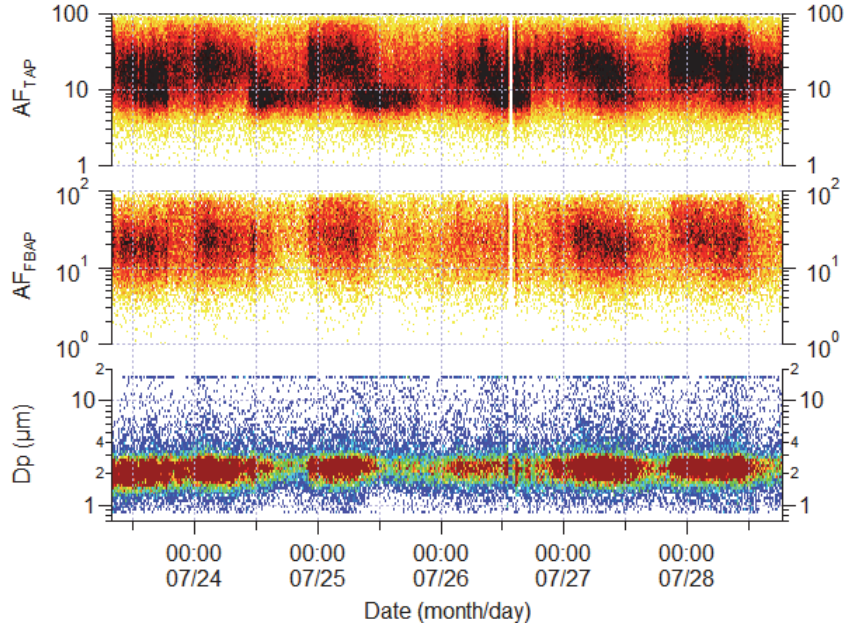

Fig. 11. Asymmetry factor (AF) data combined with fluorescence data for one selected time period in summer.

ACPD
12, 17607–17656, 2012

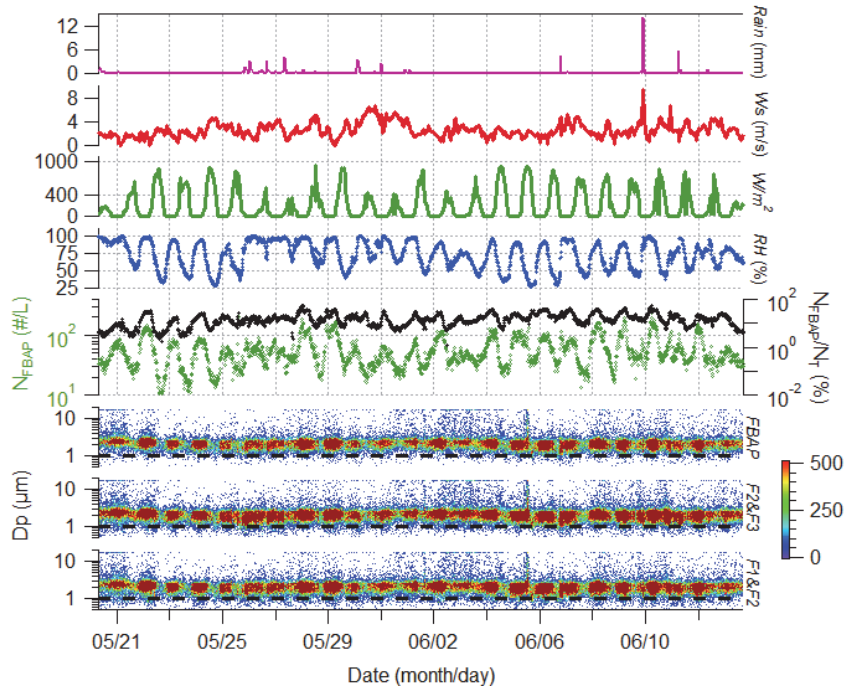

Fig. 12. WIBS-4 fluorescence data for a selected time period during spring season in comparison with meteorological data measured at the same time. The lower panels represent different combinations of fluorescent channels (F1 and F2: FL1_280 and FL2_280, F2 and F3: FL2_280 and FL2_370, FBAP: FL1_280 and FL2_370). The upper panels show from bottom to top; number concentration of FBAP (left) and ratio of FBAP to all particles (right) measured by WIBS (0.8–16 µm), relative humidity (%), global solar radiation ($W m^{-2}$), wind speed ($m s^{-1}$), precipitation (mm).

ACPD
12, 17607–17656, 2012

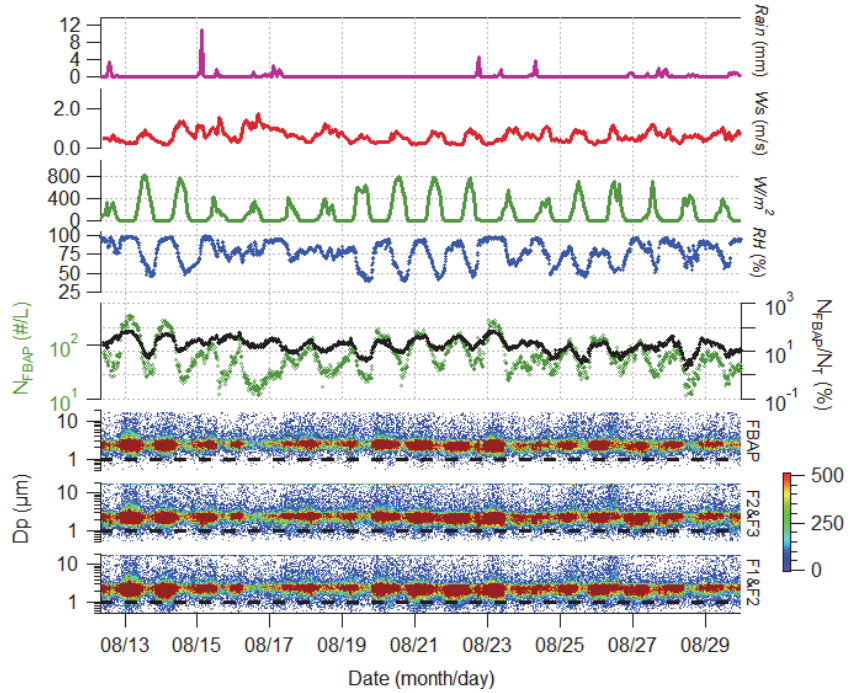

Fig. 13. WIBS-4 fluorescence data for a selected time period during summer season in comparison with meteorological data measured at the same time. The data were plotted in the same way as in Fig. 12.

ACPD
12, 17607–17656, 2012

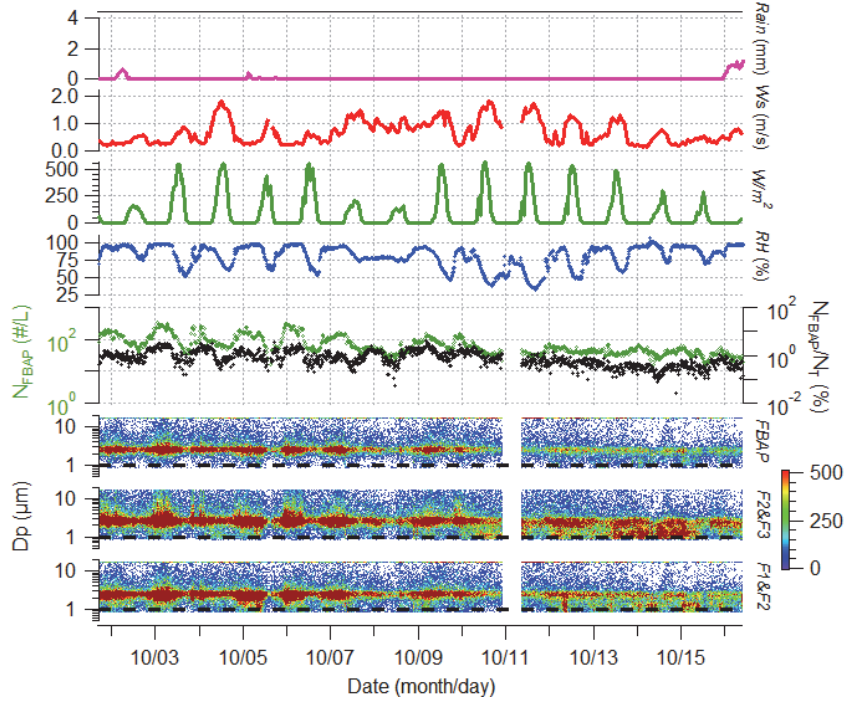

Fig. 14. WIBS-4 fluorescence data for a selected time period during autumn season in comparison with meteorological data measured at the same time. The data were plotted in the same way as in Fig. 12.

ACPD
12, 17607–17656, 2012

Fluorescent biological aerosol particles (FBAPs)

E. Toprak and M. Schnaiter

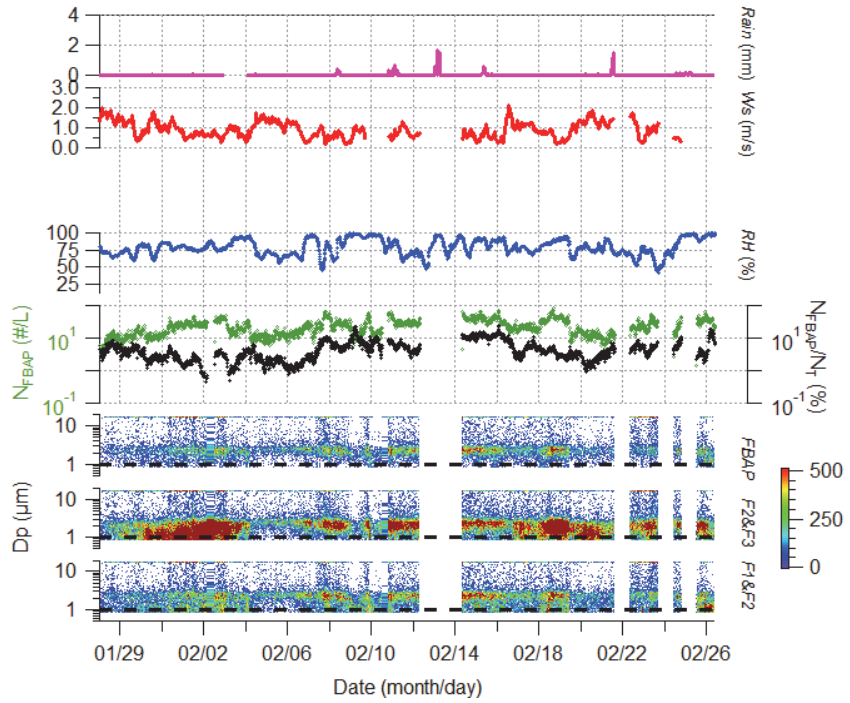

Fig. 15. WIBS-4 fluorescence data for a selected time period during winter season in comparison with meteorological data measured at the same time. The data were plotted in the same way as in Fig. 12.

ACPD
12, 17607–17656, 2012

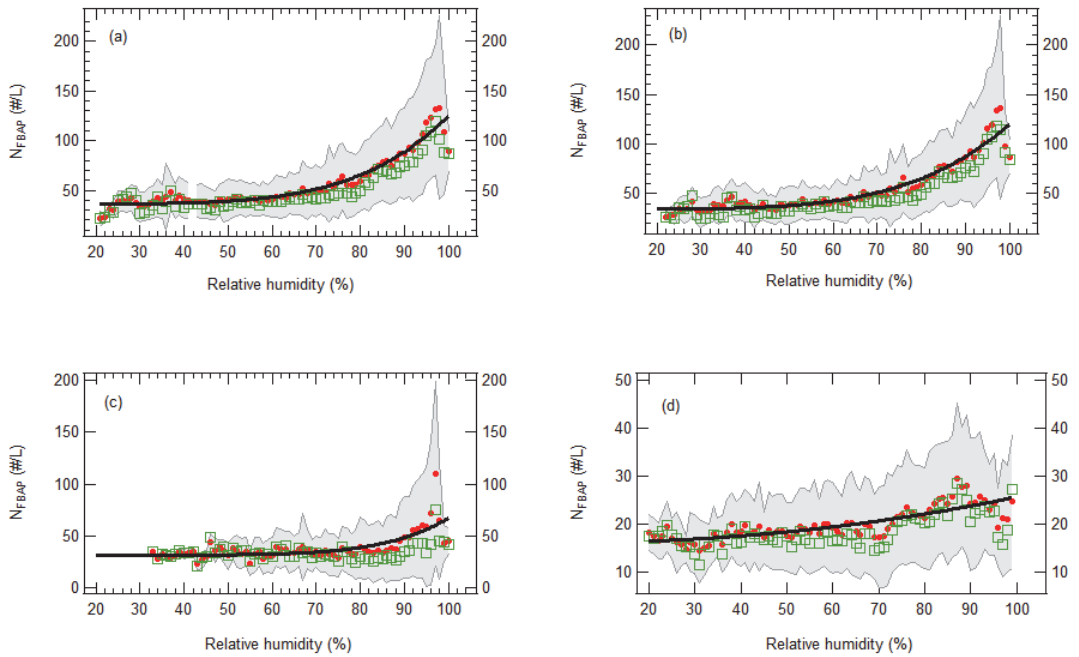

Fig. 16. Correlation of the WIBS-4 FBAP number concentrations with the relative humidity; red markers show mean FBAP concentration (N_{FBAP}, #/l), green markers show median N_{FBAP}, solid black lines represent fitted curve according to the mean N_{FBAP}, grey shaded areas represent variability of FBAP concentration as plus-minus standard deviations. Fit function; $f(x) = ax^b + c$; **(a)** spring ($R^2 = 0.924$), **(b)** summer ($R^2 = 0.911$), **(c)** autumn ($R^2 = 0.541$), **(d)** winter ($R^2 = 0.652$).

ACPD
12, 17607–17656, 2012

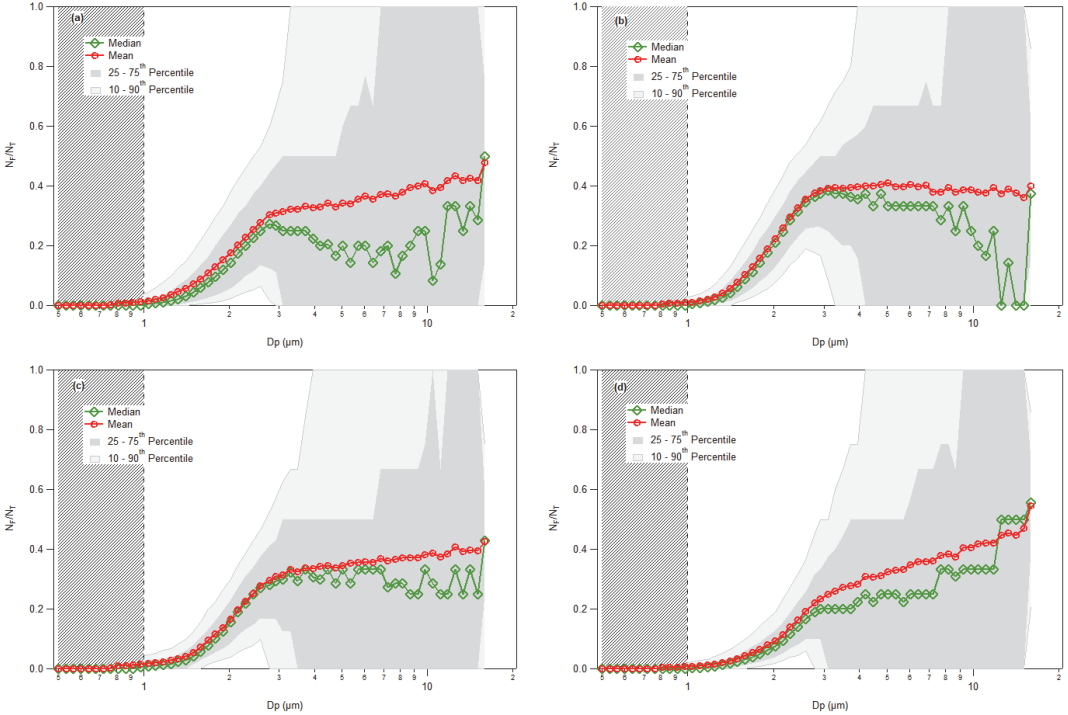

Fig. 17. Fluorescence ratio distribution for different seasons: **(a)** spring, **(b)** summer, **(c)** autumn, **(d)** winter. Left axis indicates the ratio of number of fluorescent particles to total particles for different size bins.

ACPD
12, 17607–17656, 2012